COMOTI
ROMANIAN RESEARCH & DEVELOPMENT INSTITUTE FOR GAS TURBINES

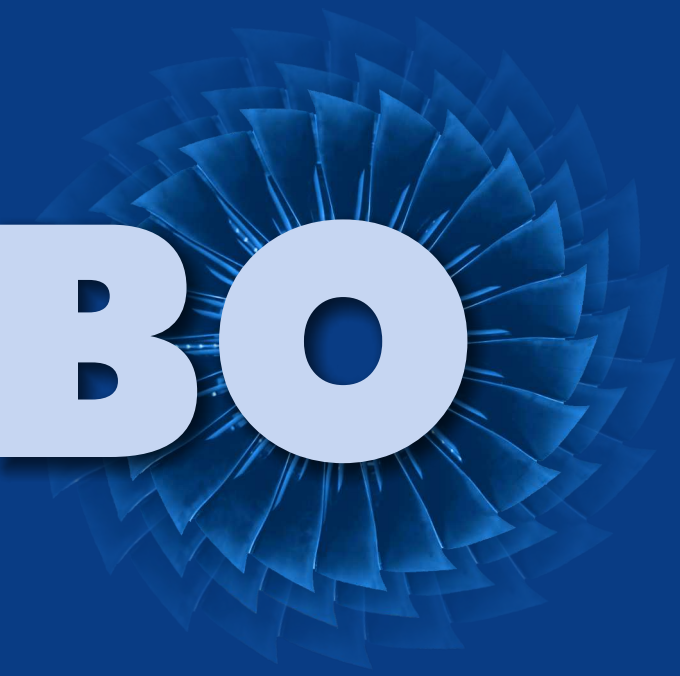

TURBO

Scientific Journal

vol. IV (2017), no. 1

CEAS

http://ceas2017.org

Aerospace Europe CEAS 2017 Conference

European Aerospace "Quo Vadis?"

(6th CEAS Air & Space Conference)

The 6th CEAS Air & Space Conference aims to promote new visions and trends in aeronautics and space science and technology according to its fundamental theme: „European Aerospace: Quo Vadis?". The Conference aims to bring together academia, research, industry, policy maker and maintenance, repair and operator stakeholders for a fruitful exchange of the latest ideas and developments in European aeronautics and aerospace.

Main objectives of the conference

- To facilitate the reunion of the main actors in European aeronautics & space environment.
- To contribute for gradualy upgrading and transforming the Conference into European Aerospace Congress.
- To encourage the young professionals and PhD students to join and contribute for an European scientific event.
- To contribute for European leadership in aeronautics & space sciencies.

Organized by:

COMOTI ROMANIAN RESEARCH & DEVELOPMENT INSTITUTE FOR GAS TURBINES

AAAR Asociatia Aeronautica si Astronautica a Romaniei

Sponsors:

esa European Space Agency

INCAS - NATIONAL INSTITUTE FOR AEROSPACE RESEARCH "ELIE CARAFOLI"

AEROSTAR S.A. GRUP INDUSTRIAL AERONAUTIC-BACAU-ROMANIA

DASSAULT SYSTEMES

MAGIC ENGINEERING

INAS power to change

ISS

Partners:

rosa

E-CAero

ECCOMAS

ERCOFTAC European Research Community On Flow, Turbulence And Combustion

ETC European Turbomachinery Conference

EUROPEAN MECHANICS SOCIETY

EUROAVIA

ROMAERO S.A.

easn

EUROTURBO

EDITORIAL

”Viziunea este arta de a vedea lucrurile invizibile” Jonathan Swift

Raportarea fiecărui om la micro si macrocosmos este adesea bazată pe indiferenţă ori pe o banală curiozitate. Dar ce uriaşă surpriză apare atunci când o privire atentă conduce la dorinţa de schimbare, de înnoire ca necesitate: curajul de a rupe bariere.

Dincolo de subiectivismul inerent, viziunea nu are legătură cu vârsta, iar frumuseţea pe care se bazează schimbarea poate duce la evoluţie: a individului, a societăţii, a omenirii.

Lumea, asa cum o cunoaștem astăzi, a cunoscut schimbări dramatice și schimbari fericite sub impactul nevoii de nou și al curiozității, a fost revoluționată de adevărați strategi în artă, în tehnică, în medicină, în politică, în fizică şi nu numai.

Pentru că timpul trece astăzi mai repede, pentru că accesul la resurse de orice fel a devenit foarte facil, viteza cu care lucrurile se petrec nu ne mai lasă timp de reflexii îndelungate. Ceea ce astăzi poate fi privit ca progres în evoluţia societală, mâine poate lua o turnură dramatică cu efecte de neoprit, pentru că viteza cu care lucrurile se întâmplă se află sub imperiul circumstanţelor economice şi politice.

Istoria culturală nu se poate imagina prin detașare de lumea vie, iar acest binom dispune de o forță progresivă, bazată pe interacțiune într-o sinteză teoretică și practică deopotrivă. Din practică derivă dezvoltarea tehnologică, ca forma de proliferare a inițiativelor, a proiectelor de cercetare, urmărind abordări majore adaptate unei experiențe de zeci de ani.

Vom continua să publicăm rezultatele cercetărilor noastre şi mulţumim celor care vor contribui la prestigiul acestei publicaţii.

Punem punct aici pentru a putea începe!

”Vision is the art of seeing what is invisible to others” Jonathan Swift

Each individual’s interaction with the micro or macrocosmos is often based on either indifference or natural curiosity. However, a closer look into things may reveal astonishing discoveries that can trigger the desire of change and renewal as a genuine necessity: the courage to break barriers.

Beyond any inherent subjectivism, perspective has nothing to do with age, while the beauty of change may ultimately pave the way to individual, social and even mankind evolution.

The world, as we know it today, has registered dramatic and welcomed changes under the impact of renewal and curiosity need, it has systematically been revolutionized by visionary minds in various domains, such as art, technical and medical sciences, politics, physics and many more others.

Today, due to a different perception of time, and also to a much more easier access to resources of all kinds, the quick pace of everyday life does not allow us enough time for extended reflection anymore. What we may perceive today as a progress in social evolution it may be tomorrow’s curse, that is, a dramatic change with unimpeding consequences due to the fact that things occur so quickly and they can be triggered by economic and political circumstances.

Cultural history cannot be conceived as separated from the natural world, and this binomial feature relies on a progressive force based on interaction in a theoretical and practical synthesis altogether. Practice induces technological development, as a form of extended initiatives and research projects, that follows major approaches adapted to dozens of years of experience.

We shall pursue publishing the results of our research activity and we do appreciate everyone’s contribution to increasing the prestige of this specialized publication.

Let’s stop here so we can begin!

Autor/Author: Elena Banea

EDITORIAL BOARD

COMOTI
ROMANIAN RESEARCH & DEVELOPMENT INSTITUTE FOR GAS TURBINES
220D Iuliu Maniu Ave., 061126 Bucharest 6, ROMANIA PO 76, POB 174
Phone: +40 021/4340198, +40 021/4340240; Fax: +40 021/4340241
E-mail: contact@comoti.ro, www.comoti.ro
Nr. Of. Com. Reg. J40/4880/1997, CIF: RO445238

TURBO
Scientific Journal

PRESIDENT:
Dr. Eng. Valentin SILIVESTRU

VICE-PRESIDENT:
Dr. Eng. Cristian CÂRLĂNESCU
Dr. Eng. Romulus PETCU

SECRETARY:
Dr. Eng. Jeni POPESCU

MEMBERS:
Prof. Dr. Virgil STANCIU
Prof. Dr. Corneliu BERBENTE
Prof. Dr. Dan ROBESCU
Prof. Dr. Sterian DĂNĂILĂ
Dr. Eng. Gheorghe MATACHE
Dr. Eng. Ene BARBU
Eng. Gheorghe FETEA
Dr. Eng. Ionuț PORUMBEL
Dr. Eng. Mircea Dan IONESCU
Dr. Eng. Lucia Raluca VOICU
Dr. Eng. Mihaiella CREȚU
Dr. Eng. Cleopatra CUCIUMIȚA
Eng. Sorin GABROVEANU

EDITOR IN CHIEF:
Prof. Dr. Lăcrămioara ROBESCU

EDITORS:
Eng. Mihaela Raluca CONDRUZ
Iulia VOINEA
Ec. Elena BANEA

ADMINISTRATIVE SECRETARY:
Eng. Mihaela GRIGORESCU

TRANSLATION CHECKING:
Dr. Eng. Paul RĂDULESCU
Laura COMĂNESCU
Oana HRIȚCU

GRAPHICS:
Victor BEȘLEAGĂ

More information regarding the scientific journal can be found at:
http://www.comoti.ro/ro/jurnalul_stiintific_turbo.html
turbojournal@comoti.ro
jeni.popescu@comoti.ro

The articles from this journal cannot be copied or republished without the editorial's board permission.

TABLE CONTENT

ADVANCED COMMUNICATION TECHNIQUES BUILT ON INTEGRATED AUTOMATION OF EXPERIMENTAL TEST BEDS

Andrei MITRU[1], Constantin VILCU[1], Adrian STOICESCU[1], Claudia BORZEA[1], Cristian NECHIFOR[1]

ABSTRACT: The paper describes a communication system within industrial environment between central processing units of the experimental test beds and a laboratory server. Execution of such a communication system requires a scientific study of the communication solutions for the test beds and the server system. The paper determines that a server software implementation will be required. During this phase, a server SCADA application and a resources distribution algorithm are required to be developed. The server hosts one SCADA application which is monitoring and controlling the experimental test beds using the communication system. The application displays in real time values for parameters, the screens containing process flow diagrams, states and processing unit control information from experimental test beds. A smart data acquisition is required to be implemented on the server system which is recording the test beds running parameters by generating data files on the server for later analysis. The server is acting as a resources distribution system for all experimental test beds. An algorithm is required to be developed on the experimental server system. The server through the algorithm is capable to associate tasks from a terminal of a test bed to another and has availability to host activities like resources consuming data acquisition and process calculation. Industrial communication security and procedures for monitoring of the server application users are required to be accomplished also. The paper includes test results within industrial environment that determines the performance for both communication system and server. The results are subject of interpretation and provides a model for future experimentation.

KEYWORDS: experimental server, smart data acquisition, communication system, resources allocation, SCADA application.

NOMENCLATURE

IED - Intelligent Electronic Device;
SCADA - Supervisory Control And Data Acquisition;
UDP - User Datagram Protocol.

1. INTRODUCTION

A supervisory control and data acquisition (SCADA) server allows an operator to remotely monitor and control the main apparatus and machines used in an automated process. A SCADA server or data concentrator collects information from the different intelligent electronic devices (IEDs) that supervise the process, and then processes the information to make it available to a remote supervisory system. The SCADA server is able to convert data between different communication protocols [1].

The paper analysis originates from a technology formulated concept which defines a supervisory control and data acquisition (SCADA) server that allows an operator to remotely monitor and control the main apparatus and machines used in an automated process. A SCADA server collects information from multiple intelligent electronic devices (IEDs) that supervise the process, and then processes the information to make it available to a remote supervisory system.

[1] National Research and Development Institute for Gas Turbines COMOTI, Bucharest, Romania

2. OBJECTIVES

The first objective for the server to be operational is to perform a study meant to identify the best solutions for obtaining a hi-speed connection between the server system and data processing test beds terminals. This first step has a crucial role in feasibility of the experimental server system.

The second objective consists in a programming environment and operating system that need to be selected for developing the experimental server application. For this objective to be fulfilled, a couple of programming environments will be taken into consideration and after a complex analysis the best option for the feasibility of the experimental server system will be selected.

The third objective is programming the application intended to be a human machine interface of the experimental test beds. After a developed inceptive version of the application software is done, it will then be always improved considering the system needs and efficiency. Feasibility of the server system will encounter a challenge by establishing a suitable communication protocol between each type of automation system of the experimental test beds and the server application.

The forth objective requires for testing the experimental server once software programming and resource distribution architecture is accomplished. This objective will first have an impact on the server system outcome by setting up of a priority for experimentation of the communication system. Secondly, feasibility will be outlined when the server application will be tested within the communication system of the experimental test beds.

The outcome of the experimental server will be concluded by system resources distribution assessment during tests. An analysis is recommended to be made concerning the behavior of the communication system when critical events occurs like emergency shut down of one or multiple test beds.

3. COMMUNICATION ARCHITECTURE

3.1. The experimental server desired performances

The experimental server system is intended to be capable of associating tasks from a terminal of a test bed to another and will have availability to host activities like resources consuming data acquisition in real time and process calculation [2].

A smart data acquisition procedure is intended to be implemented on the experimental server system. The procedure will generate data files on the server for later interpretation and processing at request from the running experimental test beds [3].

The server equipped with custom made software displays in real time the parameters from the test beds. The HMI (human-machine interface) provides a more addressable communication with the server operator through screens containing process flow diagrams and values for parameters, states and processing unit control information.

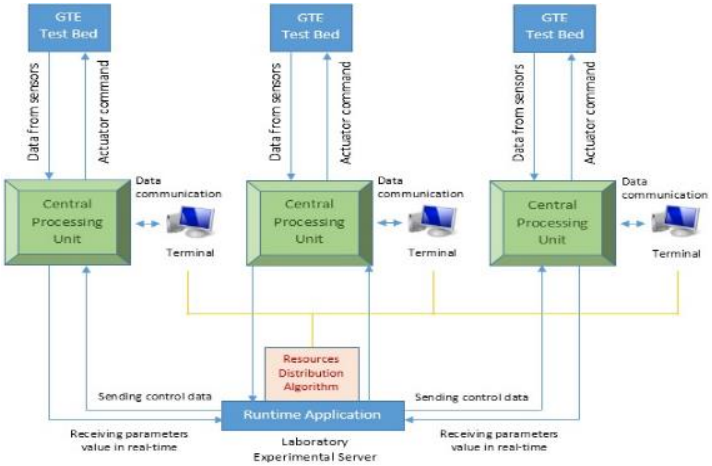

Fig. 1 Schematic communication diagram of the experimental server serving the test beds

Experimentation will assume testing limits of and functionality of the communication system seen in Fig.1 for high speed bladed machines prototypes within industrial environment.

For any operation sequence of any test bed with its central processing unit connected to the SCADA system, the developed running application permanently monitors the values of the technological parameters signalizing optically and acoustically any change from the technologically imposed values.

The technological diagram screen is the first screen to appear on the SCADA application depending on human selection inside application regarding which test bed is to be operated.

Warning messages will appear on the SCADA application for the parameters whose values do not allow the start-up of a certain test bed. Until those conditions from the messages are fulfilled the test bed cannot be started.

Non-critical messages will be triggered by certain events during operating state of any test beds and will warn the human operating the SCADA system. In case of failures, all safety protections for the test bed to perform automatic stop are transmitted into its central processing unit which communicates with the SCADA system, and human operator will be notified of the failure and its causes.

A clear hierarchy within the test bed SCADA systems will be set. According to this hierarchy, server application architecture and interoperability follow. Aspects such as user authentication, user activity recording, testing and fixing security breaches are also important [1].

The desired performances also consist by researching together how advanced interoperability and security could become for this type of experimental product.

Multiple stations which own high speed bladed machines could receive this experimental server as a command, monitoring and resources distribution center.

3.2. Experimental test beds infrastructure and resources allocation concept

The software system within each terminal of the experimental test beds includes a data acquisition, processing and recording system for the running parameters and states delivered by a central processing unit.

Each data processing terminal communicates with a central processing unit. Implemented software supported by a local terminal allows an accurate and full control of the test bed through the central processing unit. The experimental server system is capable to communicate data with the central processing unit of each test bed through a certain communication protocol depending on the automation system [2].

Tasks representative for test bed experimentation such as heavy calculation, detailed graphic with numerous parameters, heavy data acquisition will be supervised and shared within the SCADA systems network.

Some of these projects like testing gas turbine engines in various working conditions will improve results through a one entity controlling server.

During experimentation phase a test bed SCADA system will be intentionally loaded with tasks so that the performance data parameters from the network system will be analyzed.

Sharing resources is important to ensure that the communication system efficiently serves all test bed terminals. There are many ways to share resources. Given that resources are limited, the communication system needs to enable terminals to efficiently share operations among them.

The resources allocation concept is to implement and always improve an algorithm which finally will prove efficient after the project test bed experimentation.

4. RESULTS

Having the purpose to measure the data transmission performance, there were used two terminals which are connected through Wi-Fi hardware on both ends. These terminals have established a Wi-Fi connection in which the first terminal acted as the experimental server and the other acted as a test bed terminal.

For obtaining the experimental results regarding the data transmission performance a specialized application has been used. The name of the application is Jperf and it has run on both terminals simultaneously [4]. This application generated data traffic between the server and the test bed terminal.

Before data transmission to be initiated, the test bed has been put into service. The communication path between the two terminals has been purposely arranged in such of manner that radio waves transmission were passing through the experimental test bed. Also, welding procedures were taking place near the test bed into the hall. In this manner, industrial environmental conditions were fulfilled.

During applying of various operating schemes to the test bed, Jperf application was initialized on the experimental server. Also, the Jperf application was started in client mode on the test bed terminal. Jperf application has generated a 1 Mbps traffic through 500 bytes UDP datagrams during 200 seconds which was a imposed amount of time.

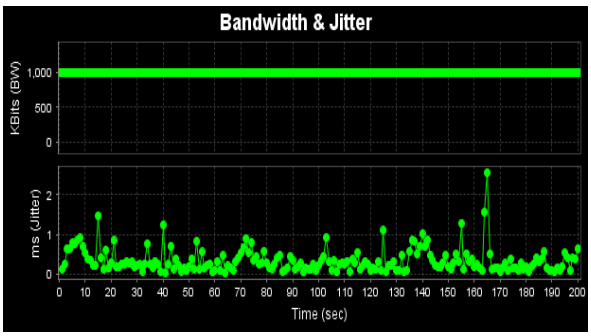

Fig. 2 Data transmission and delaying analysis for the experimental server

During the 200 seconds experimental time, 1Mb/s data packets were sent through the Wi-Fi connection into the industrial environment. From the experimental datagram seen in Fig. 2 results that the highest data delay is at almost 3 msec from the moment it has been sent. From the experimental results it is concluded that no data packets were lost during experiments.

5. CONCLUSIONS

The key issues taken into consideration by this paper, and hence open issues for research (also extensively documented in literature [1], [2], [3]), are:

• Speed and efficiency are critical factors to be considered, because of the very large number of parameters to be acquired with high sampling rate during the testing of gas turbines, via a multitude of sensors (specific requirement of the experimental test beds).

• Interoperability between multiple vendor-provided central processing units for multiple test beds available and a single server.

• Security issues, which are an emerging challenge in the SCADA networks, which were not initially designed for security. Failure of security for a control system driving a hi-speed turbine operating in excess of 10.000 rpm can have disastrous consequences.

Starting from this technology formulated concept, the paper scope is to make an analysis on test results from a experimental server system that hosts one programmed SCADA application which will be monitoring, controlling and act as a resources distribution interface for multiple experimental test beds, using hi-speed network links to all the terminals that belong to the experimental test beds.

The test results are showing that there are no data loss and the maximum delay of 3 ms is considered acceptable.

ACKNOWLEDGEMENT

This work was carried out within “Nucleu” Program TURBO 2020, supported by the Romanian Minister of Research and Innovation, project number PN 16.26.07.02.

REFERENCES

[1]. Yardley T., “SCADA: issues, vulnerabilities, and future directions” https://www.usenix.org /system/files/login/articles/258-yardley.pdf.
[2]. Nan C., Eusgeld I., Kröger W., 2013, “Analyzing vulnerabilities between SCADA system and SUC due to interdependencies”, Reliability Engineering & System Safety
[3]. Davidson E. M. et al., 2006, “Applying Multi-Agent System Technology in Practice: Automated Management and Analysis of SCADA and Digital Fault Recorder Data”, IEEE transactions on power systems, vol. 21, no. 2.
[4]. https://sourceforge.net/projects/jperf/.

DATA RECORDER SYSTEM FOR MAINTENANCE TO ROTARY BLADE MACHINES – "HolderPPS"

Filip NICULESCU[2], Constantin VILCU[2], Alexandru GAZDAC[2], Claudia BORZEA[2]

ABSTRACT: The HolderPPS system presented in this paper falls into the category of recording systems created for the proactive maintenance of rotary bladed machines. Based on an innovative architecture, the Holder-type system contributes to machine equipment diagnosis and to early warnings on potential flaws in the functioning of the machine. The system is able to determine, in real time, the causes of the warnings and of the emergency stops of the machine, in order to avoid any potential failures, or the rendering inoperative of the machine. These causes can be established by monitoring the critical parameters of the machine: vibrations, temperature, and quality of the lubricating oil. As such, data collected and processed on the basis of algorithms relating to high speed mechanical systems, allow local diagnosis of the current state of the machine, or data transfer, by remote connection, to a laboratory where an off-line analysis can be performed.

KEYWORDS: Preventive and Predictive Maintenance, Reliability of rotary blade machines, Data Recorder System

NOMENCLATURE

APN – Access **P**oint **N**ame;
PPS – Predictive / **P**roactive **S**ystem;
HolderPPS – Data Recorder System for Proactive Maintenance to Rotary Blade Machines);
IQ sensors – **I**ntelligent **Q**uality sensors;
PLC – Programmable **L**ogic **C**ontroller;
RBM – **R**otary **b**lade **M**achine;
SCADA – Supervisory **C**ontrol **A**nd **D**ata **A**cquisition;
USB – Universal **S**erial **B**us;

1. INTRODUCTION

The activities carried out for a piece of equipment or for the rotary bladed machine so as to allow them to perform functions that they have been initially designed for, play a critical role in the smooth functioning of the products for a period at least equal to that provided by the manufacturer. A more efficient maintenance strategy would assume limiting downtime and detecting, as accurately and as early as possible, the potential causes of future problems, and also simplifying, as much as possible, work taken forward in order to address issues and reduce their impact on the machine. The main types of maintenance strategy are: Corrective (reactive); Planned; Preventive; Predictive; Proactive, [2]. The evolution of maintenance over time is shown in Fig. 1. [1]. Proactive maintenance, based on reliability and risk, has marked the shift to reliable-centred maintenance, at the beginning of the century. These two types of maintenance are based on equipment (+) machine state parameters (+) process state parameters (+) environment (+) operating staff. Reliable-centred maintenance ensures that, on one hand, equipment availability has been maximized, and, on the other hand, that operating costs have been minimized and therefore investment has become profitable, [3]. At the same time, this type of maintenance provides the necessary conditions to ensure the greatest durability of the equipment, by making rotary bladed machines more and more environment-friendly.
by extremely fast modules, connected to a central unit, that can be further on connected to a display unit.

[2] National Research and Development Institute for Gas Turbines COMOTI, Bucharest, Romania

The "HolderPPS" system becomes operational in the proactive maintenance of rotary bladed machines, as it authorizes uninterrupted and dynamic tracking of the operating state of all the elements of the machine's mechanical system. Thus, under the conditions specific to the industrial process in which the machine operates, early defects can be rapidly identified and tackled. Dedicated software installed in the real-time controller unit can create databases while processing data, so that centralized management of the machine can be implemented, which makes possible the quick identification and tackling of any potential defect. This is an efficient way to detect defects at an early stage, and to deal with them in a given time interval so as to avoid a time-consuming shutdown of the bladed machine, at inappropriate moments. If the results of the bladed machine monitoring activity are kept in a database, as mentioned earlier, a history of all the tracking records can be created, by gathering useful data for a periodic analysis of the underlying defect causes. Thus, measures can be taken, so as to avoid future occurrences of any defect. Such an approach to problem identification and solving is the proactive one. This approach can lead to significant medium and long term economies of scale.

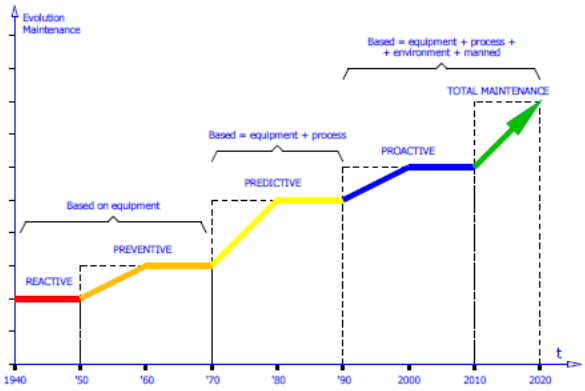

Fig. 1 – The evolution of maintenance in time

1. HolderPPS COMPONENTS

The *HolderPPS* system consists of sensors and of a mobile box with electrical connections. The box includes monitoring, acquisition, processing and storage components. The contact and/or non-contact sensors will be connected to the main box via cables with water and dust resistant connectors. Data stored in the system shall be sent to a cloud storage platform, by means of a modem, or straight to the analysis and interpretation server in the laboratory.

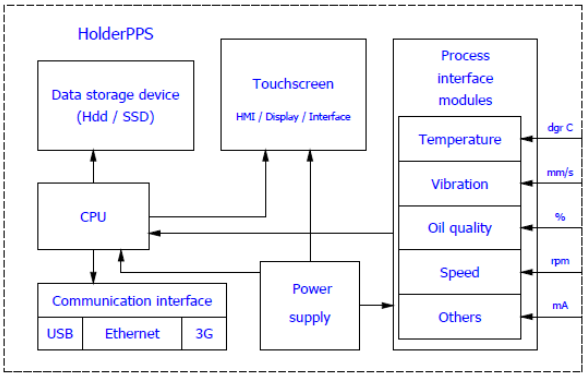

Fig. 2 – Block diagram for the HolderPPS recording system

Bladed machine parameters shall be measured by the sensors, which can be contact or non/contact, depending on their position relative to the position of the machine: while non-contact sensors are installed in the proximity of the machine, contact sensors are installed directly on the machine. Parameters will then be acquired

The block diagram in Fig. 2 shows the main components of the HolderPPS system:

- the sensitive screen, where data can be viewed and commands can be done;
- the CPU microcontroller, that processes data according to algorithms created at a previous stage;
- the power supply, that provides system components with the energy needed;
- the storage device, that provides a record of the data obtained while connecting the system to the installation monitored;
- the communication interface, which ensures data transfer and communication to the local system or distance communication;
- the modules that ensure the interface with the process; they provide physical parameters conversion to electrical data, that can then be processed and stored.

The development of this recording system has been achieved using a modular, RIO-type platform, provided by National Instruments, which consists of a central unit and several data acquisition modules. *HolderPPS* system related electrical box is equipped shown in Fig. 3.

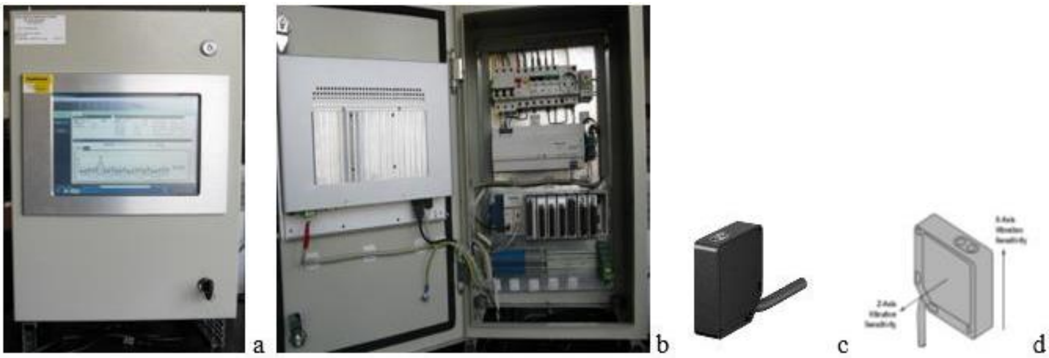

Fig. 3 –Equipment of the HolderPPS electrical box

a) Front panel; b) Counter-panel box; c) QM42VT1 sensor; d) Two axes vibration sensor

2. MEASUREMENTS

Measurements and recordings have been made on one of the compressors, through direct connection (via Ethernet), of the *HolderPPS* system to the *PLC* of the compressor. These measurements are used afterwards for the „off-line” analysis of the normal operating mode and then the diagnosis of the rotary bladed machine. Out of the various parameters recorded, the variation over time, of rotor vibrations, on each of the four compression stages is shown in Fig. 4. Albeit different as value $VR_i \in (9 \div 16)$, [mm/s], rotor vibrations present a linearity which indicates the proper functioning of the bladed machine.

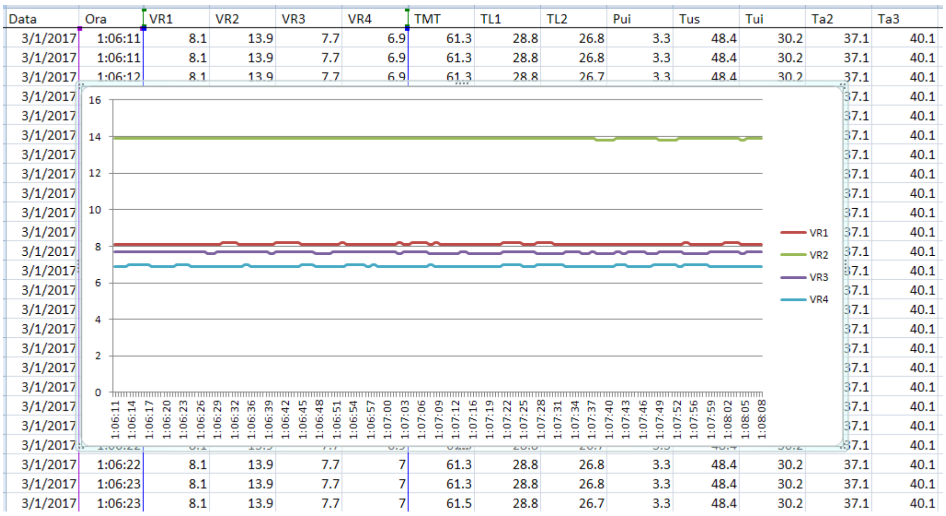

Fig. 4 – Records indicating the variation of rotor vibrations, for a centrifugal compressor in four compression stages

Fig. 5 illustrates variation over time of one of the state variables (i.e. temperature), for the lubricating oil used in the machine, as well as for the working fluid (i.e. air), before and after each compression stage. The values of temperature measurement results indicate the proper functioning of the machine, which is also ensured by keeping the variation in temperature intervals linear.

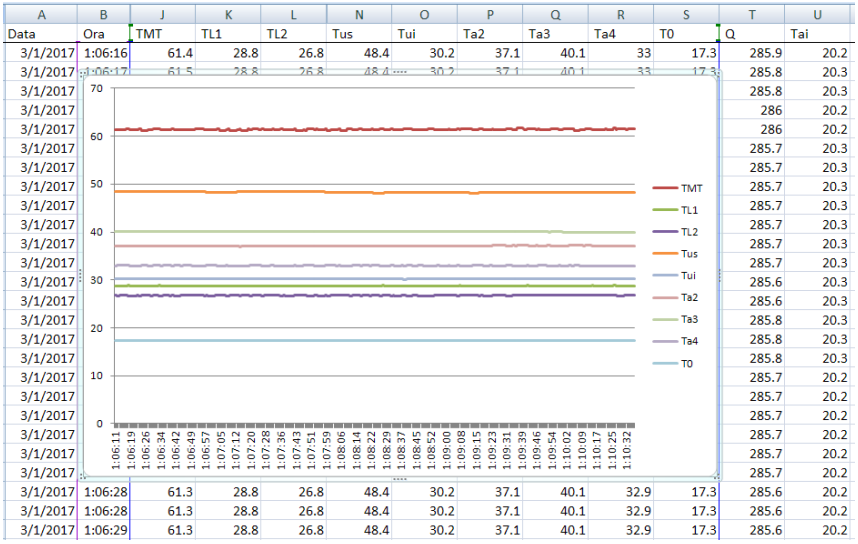

Data	Ora	TMT	TL1	TL2	Tus	Tui	Ta2	Ta3	Ta4	T0	Q	Tai
3/1/2017	1:06:16	61.4	28.8	26.8	48.4	30.2	37.1	40.1	33	17.3	285.9	20.2
3/1/2017	1:06:17	61.5	28.8	26.8	48.4	30.2	37.1	40.1	33	17.3	285.8	20.3
3/1/2017											285.8	20.3
3/1/2017											286	20.2
3/1/2017											286	20.2
3/1/2017											285.7	20.3
3/1/2017											285.7	20.3
3/1/2017											285.7	20.3
3/1/2017											285.7	20.3
3/1/2017											285.7	20.3
3/1/2017											285.7	20.3
3/1/2017											285.6	20.3
3/1/2017											285.6	20.3
3/1/2017											285.8	20.3
3/1/2017											285.8	20.3
3/1/2017											285.8	20.3
3/1/2017											285.7	20.2
3/1/2017											285.7	20.2
3/1/2017											285.7	20.2
3/1/2017											285.7	20.2
3/1/2017											285.7	20.2
3/1/2017											285.7	20.2
3/1/2017	1:06:28	61.3	28.8	26.8	48.4	30.2	37.1	40.1	32.9	17.3	285.6	20.2
3/1/2017	1:06:28	61.3	28.8	26.8	48.4	30.2	37.1	40.1	32.9	17.3	285.6	20.2
3/1/2017	1:06:29	61.3	28.8	26.8	48.4	30.2	37.1	40.1	32.9	17.3	285.6	20.2

Fig. 5 – Records of temperature variation on a four-stage centrifugal compressor

3. CONCLUSIONS

The monitoring and recording *HolderPPS* system is able to perform continuous and/or periodic recordings, on a short term or long term basis. It is a portable system, which can be used, when necessary, in the different locations of the *RBM*. The *HolderPPS* system is intended particularly for the analysis of those rotary bladed machines which have not yet implemented the SCADA automation system. The *HolderPPS* system can be used for recording the state variables of the machine for short periods of time (predictive maintenance investigations), as well as for recording the operational parameters of the machine, for longer periods of time (proactive maintenance).

ACKNOWLEDGEMENT

This work was carried out within "Nucleu" Program TURBO 2020, supported by the Romanian Minister of Research and Innovation, project number PN 16.26.03.01.

REFERENCES

[1] Ungureanu M.; 2015 "Maintenance of Mechanical System" course, București;
[2] Câmpan M., Arghir M.; 2013 "Studies and researchers of equipment maintenance",The 13th National Conference, *Professor Dorin PAVEL – founding member of the Romanian Hydroelectric Sector*, Sebeș;
[3] T. Munteanu, G. Gurguiatu; 2009 „Reliability and quality in electrical engineering", Lecture notes, Galați University Press;
[4] Scheianu D.,Le T.; 2013, "Preventive maintenance program and novel techniques to reduce downtime and increase operating efficiency at distributed cogeneration facilities" IDEA Conference, San Diego;
[5] Williams M., Burch R., Krenek D.; 2012 "Utilizing Equipment Data for Proactive Asset Management", Gas Machinery Conference, Austin, Texas;
[6] *** *Performance Prediction and Simulation of Gas Turbine Engine Operation for Aircraft, Marine, Vehicular, and Power Generation*, RTO Technical Report, TR-AV-036, February 2007;
[7] *** *Predictive Maintenance Program*, Predictive Maintenance-Facility, Ground Support Equipment, pp 1, Technique OPS-13 https://oce.jpl.nasa.gov/practices/ops13.pdf;

SOLIDIFICATION SEGREGATION IN CMSX-4 SUPERALLOY: EXPERIMENTS AND SIMULATION PREDICTIONS

Gheorghe MATACHE[3], Alexandru PARASCHIV[3], Cristian PUȘCAȘU[3], Raluca CONDRUZ[3]

ABSTRACT: The segregation degree of alloying elements during solidification in as-cast CMSX-4 single-crystal superalloy was investigated. The elemental partition coefficients calculated using the results of experimental measurements of local compositions and predicted by thermodynamic calculation in multicomponent alloys have shown the tendency of the elements to segregate either into the dendrites (W, Re) or in the interdendritic regions (Al, Ti, and Ta). Among the alloying elements Re has the strongest tendency to segregate. It was found a good agreement between the experimental and simulation prediction results, as well as compared with an analytical model. By thermodynamic calculation it was established the influence of superalloy chemistry on the elemental segregation during solidification.

KEYWORDS: superalloy, segregation, partition coefficient, simulation

1. INTRODUCTION

The gas turbines performances particularly rely on the outstanding properties of Ni-based superalloys at high temperatures. The chemistry of different Ni–based superalloy generations designed to produce single-crystal or columnar structure blades includes a high content of refractory elements (W, Ta, Re, and Ru) and a lower content of Cr, Co, and Mo compared with the previous alloy generations that exhibit equiaxed grains. Most of these alloys are designed or optimized to generate a high fraction of strengthening γ' phase [1], good mechanical properties at high temperatures, and resistance to oxidation. For this purpose, alloying elements such as Al, Ti, and Ta are still used with a tendency to increase the Al content to the detriment of Ti content. Most of the modern superalloys have the disadvantage of very high density, poor corrosion resistance in bare condition and are very expensive [2]. It was previously shown that the increase of Ta and Cr content in single-crystal superalloys decrease the segregation tendency of high-density elements (W, Re). The composition must be balanced to avoid other undesired defects development knowing that Ta increases the eutectic fraction and too high content of Cr leads to the formation of brittle topological closed packed (TCP) phases [3].

The introduction of directional solidification in order to avoid the transverse grain boundaries led to the decrease of the content of the alloying elements (B, C) which have been commonly used to strengthen the grain boundaries in equiaxed structures [4]. However, recent papers have shown that low contents of Zr and B are suitable to ensure a good castability of these alloys [5]. The single-crystal superalloy development is usually controlled by the thermal gradient (G) and solidification rate (V). Recent papers have shown that higher thermal gradients generate smaller dendrite arm spacing, refined microstructure and a reduced level of segregation [6, 7]. In the development or optimization of single-crystal superalloys with high refractory elements content there is a major concern to decrease or avoid the tendency to generate casting defects due to the preferential segregation of alloying elements either in the dendrites or in the interdendritic areas [8, 9]. Other authors have shown that the strong segregation tendency of high-density refractory elements generates a density inversion occurrence at the liquid/solid interface in the mushy zone [10]. Since the structure homogeneity of materials is of paramount importance to generate appropriate high temperature properties, the purpose of this paper is to investigate the elemental segregation in as-cast CMSX-4 single-crystal superalloy by simulation predictions and experiments.

[3] National Research and Development Institute for Gas Turbines COMOTI, Bucharest, Romania

2. MATERIAL AND PROCEDURES

The experimental investigation of the segregation was performed on single-crystal CMSX-4, representative for the second generation of superalloys. The samples were cut from rods produced by directional solidification using Bridgman method with a thermal gradient of 3 $K \cdot mm^{-1}$ and a solidification rate of 3 $mm \cdot min^{-1}$ Microstructural qualitative and quantitative analyses were done using a scanning electron microscope (SEM) Inspect F50 and by energy dispersive spectrometry (EDS) - EDAX. Solidification path prediction was simulated by thermodynamic calculations in multicomponent, multiphase alloys using Pandat™ software (a trademark of CompuTherm LLC) based on CALPHAD method and the latest thermodynamic database for Ni alloys (PanNi2017_TH).

3. RESULTS AND DISCUSSIONS

The typical as-cast microstructure of modern superalloys with low C content designed for single-crystal blades or vanes development consists of cuboidal γ' phase precipitated into the γ matrix in dendrites and in the interdendritic areas, islands of coarse γ' and different fractions of γ-γ' pools in the interdendritic areas. The γ' size in the dendrites is finer and more regular in shape than in the interdendritic regions. The difference in size and shape of γ' precipitates is governed by the growth kinetics in correlation with the segregation level of alloying elements and by the interaction between them as demonstrated for Re [11]. The high level of structure segregation is governed by the redistribution of the alloying elements at the solid/liquid interface during solidification and by the reduced diffusivity of the refractory elements. As a result there are significant differences in the chemical composition of the dendrites and the interdendritic areas leading to different lattice parameter mismatch and to residual stresses due to the different shrinkage conditions during cooling. Qualitative analysis by EDS of the investigated CMSX-4 alloy highlighted strong segregated structures. The surface distribution has shown that the high-density refractory elements (W, Re, and Co) are preferential distributed in dendrites while the γ' forming elements (Al, Ti, and Ta) are mainly segregated in the interdendritic regions. The segregation degree is commonly expressed by the partition coefficients ($k_{S(i)}$) of the elements (Eq. 1) where $C_{D(i)}$ is the concentration of the element (i) in dendrite, and $C_{I(i)}$ is the concentration of element (i) in the interdendritic areas.

$$k_{s(i)} = \frac{C_{D(i)}}{C_{I(i)}} \tag{1}$$

The partition coefficients signify the tendency of the alloying elements to segregate in the dendrites ($k_{S(i)} > 1$), or in the interdendritic areas ($k_{S(i)} < 1$). The partition coefficients were calculated based on the local chemical composition measured by EDS in the dendrite core (C), dendrite arms (DA) and in the interdendritic regions (IR) as summarized in Table 1.

Table 1. Partition coefficients calculated for as-cast CMSX-4 alloy based on experimental results

k_S	Al	Ti	Cr	Co	Ni	Ta	W	Re	Mo
k_S (C/IR)	0.91	0.78	1.00	1.09	0.89	0.89	1.18	1.40	1.12
k_S (SA/IR)	0.93	0.83	1.00	1.07	0.98	0.91	1.15	1.32	1.09
k_S (C/SA)	0.99	0.94	1.02	1.02	1.00	0.97	1.03	1.05	1.03

The results in Table 1 show that the elements that usually segregate in the interdendritic regions (Al, Ti, and Ta) exhibit partition coefficients less than 1 calculated between the dendrite cores, k_S (C/IR), or the secondary dendrite arms, k_S (SA/IR), and the interdendritic regions. The refractory elements (W, Re) that segregate in the dendrites have in both cases partition coefficients higher than 1. It was noticed that Re segregate the strongest. All other elements are almost neutral having partition coefficients around the unity. Previous work has shown that the partition coefficients exhibit a linear variation as a function of secondary dendrite arms spacing (SDAS) with a positive slope for W and Re, and a negative one for Ti, Al, and Ta [12]. A peculiarity of the segregation tendency highlighted by the experimental results is that the segregation level in the secondary dendrite arms is less pronounced than that in the dendrite cores. The partition coefficients calculated between the cores and secondary dendrite arms, k_S (C/SA) in Table 1, demonstrate this behaviour. These results are due to the partition of alloying elements at solid/liquid interface during solidification: as the solidification advances the secondary dendrite arms grow into interdendritic areas depleted in refractory elements and enriched in Al, Ti, and Ta, resulting lower partition coefficients for refractory elements (W, Re) and closer to unity for those of Al, Ti, and Ta.

Solidification path calculation using Pandat software for both equilibrium and non-equilibrium conditions (Scheil model) allow the calculation of chemical compozition of the phases as a function of solid fraction, and the calculation of the composition at solid/liquid interface. Based on the solidification path results calculated for the tipical composition of the investigated alloy partition coefficients (k_I) can be calculated as the ratio between the concentration of the elelments in the solid (C_S) and liquid (C_L) phases at a given fraction of solid. Table 2 summarize the partition coefficients calculated for CMSX-4 superalloy based on the experimental results for single-crystal (SX) and equiaxed structures (EQX), simulation predictions in Pandat at the 1% fraction of solid and using the analytical model established by Hobbs et al. [10].

Table 2. Partition coefficients for CMSX-4 superalloy calculated by different methods

Method	k_S (Al)	k_S (Cr)	k_S (Co)	k_S (Mo)	k_S (Ta)	k_S (W)	k_S (Re)
Analytical	0.92	1.04	1.05	0.35	0.77	1.15	1.37
Experimental (SX)	0.91	1.00	1.09	1.12	0.89	1.18	1.40
Experimental (EQX)	0.95	0.95	1.07	1.03	0.87	1.22	1.53
Pandat prediction	0.87	0.81	1.12	0.64	0.78	1.08	1.52

These results show that excepting the Mo there is a good agreement between the used methods and allow the use of simulation predictions as an alternative rapid assessment of the influence of changes in the chemical composition on the segregation of elements in the superalloys. The much lower level of partition coefficient of Mo calculated using the analitical model compared with the experiments can be explained by the lower level of Mo in CMSX-4 superalloy (0.6%) than in the alloys used to estblish the model. The same reason is for Pandat simulation which uses analitical models too. Since in the superalloys of practical interest deviations from the tipical composition induce changes in phase transformation points and solidification path, additional calculations of partition coefficients were performed using Pandat in order to evaluate the influence of alloying elements content on the segregation tendency in the CMSX-4 superalloy. The results summarized in Table 3 show the influence of elements to the increase (↑), decrease (↓) or have no significant influence (~) on the segregation behaviour of the alloying elements.

Table 3. Influence of alloying elements on the segregation in CMSX-4 superalloy

	Re	W	Al	Ti	Ta	Co	Cr	Ni
Re	↓	~	↑	↑	↑	~	~	~
W	~	↑	↓	↓	~	~	↓	~
Mo	↓	↓	↓	↓	↓	~	↓	~
Ta	~	↑	↓	↓	↓	~	↓	~
Co	↓	~	↓	~	↑	~	↓	~
Cr	↓	↓	~	↑	↓	↑	↓	~

Additions of Mo, Co, Cr diminishes the segregation of Re. Of these elements Co have the strongest influence on Re segregation decrease but it did not influence the distribution coefficients of W. Cromium simultaneously influence the distribution coefficients of Re and W downwards and therefore Cr is present in the composition of all superalloys. The segregation of elements that are partitioned in the interdendritic regions (Al, Ti, and Ta) are also influenced by the content of other alloying elements. Mo and Ta itself simultaneously decrease the segregation level of the three elements. All the other elements have a positive influence on some of the elements that compose the γ' phase. The partition coefficients of Co, Cr, and Ni are influenced to a very small extent by the content of all other alloying elements and are therefore these are considered to be neutral in terms of the segregation level. The pronounced segregation of alloying elements generates a high compositional gradient across the superalloys structure that must be eliminated or reduced to a great extent prior introduction to service [13].

4. CONCLUSIONS

The as-cast CMSX-4 single-crystal superalloy exhibits a strong segregated structure. The segregation tendency of the alloying elements was assessed by the partition coefficients calculated using experimental results and Pandat predictions of the solidification path. A good agreement was found between experiments, simulation predictions and an analytical model. All the methods have shown that in the investigated alloy, Re and W are particularly distributed into the dendrites while γ' forming elements (Al, Ti, and Ta) are distributed into the interdendritic regions.

It was particularly noted that Re have the highest partition coefficient and therefore the highest segregation tendency in CMSX-4 superalloy with both single-crystal and equiaxed structure.

The experimental results have shown that Re and W are segregated much stronger in the dendrites core than in the secondary dendrite arms due to the solidification path into the mushy zone depleted in refractory elements.

Using the Pandat predictions on the distribution of the alloying elements at the solid/liquid interface was performed a broad analysis of the influence of alloying elements on the segregation tendency in CMSX-4 alloy. It was shown that the increase of Mo, Co, and Cr diminishes the segregation level of Re, while Mo and Ta itself simultaneously diminish the segregation of Al, Ti, and Ta. Co, Cr, and Ni are influenced to a very small extent by the other alloying elements and are considered neutral in terms of segregation tendency.

ACKNOWLEDGEMENT

This work was carried out within "Nucleu" Program TURBO 2020, supported by the Romanian Minister of Research and Innovation, project number PN 16.26.04.02.

REFERENCES

[1]. Caron P.; 2000, High γ' solvus New Generation Nickel-based Superalloys for Single Crystal Turbine Blade Applications, in *Superalloys 2000*, (ed. T.M. Pollock et al.), 737–746
[2]. Logunov A.V., Shmotin Yu.N., Danilov D.V.; 2015, Methodological Fundamentals of Computer-Assisted Designing of Nickel-Based Superalloys, *Russian Metallurgy*, 13, 1053-1059
[3]. Feng Q., L.J. Carroll, and T.M. Pollock, 2006, Solidification Segregation in Ruthenium-Containing Nickel-Base Superalloys, *Metall Mater Trans A*, 36A, 1949–1962
[4]. Ardakani M.G., D'Souza N., Wagner A., Shollock B.A., McLean M.; 2000, Competitive Grain Growth and Texture Evolution during Directional Solidification of Superalloys, in *Superalloys 2000*, (ed. T.M. Pollock et al.), 219-228
[5]. Grodzki J., Hartmann N., Rettig R., Affeldt E., Singer R.F.; 2016, Effect of B, Zr, and C on Hot Tearing of a Directionally Solidified Nickel-Based Superalloy, *Metall and Mat Trans A*, 47, 2914-2926
[6]. Wang F., Ma D., Bogner S., A. Buhrig-Polaczek; 2016, Comparative Investigation of the Downward and Upward Directionally Solidified Single-Crystal Blades of Superalloy CMSX-4, *Metall and Mat Trans A*, 47, 2376-2386
[7]. Zhao X., Liu L., Yu Z., Zhang W., Zhang J., Fu H.; 2010, Influence of directional solidification variables on the microstructure and crystal orientation of AM3 under high thermal gradient, *J Mater Sci*, 45, 6101–6107
[8]. Karunaratne M.S.A., Cox D.C., Carter P., Reed R.C.; 2000, Modelling of the microsegregation in CMSX-4 Superalloy and its homogenization during Heat Treatment, in *Superalloys 2000*, (ed. T.M. Pollock et al.), 263–272
[9]. Ganesan M., Dye D., Lee P.D.; 2005, A Technique for Characterizing Microsegregation in Multicomponent Alloys and Its Application to Single-Crystal Superalloy Castings, *Metall Mater Trans A*, 36A, 2191-2204
[10]. Hobbs R.A., Tin S., Rae C.M.F.; 2005, A Castability Model Based on Elemental Solid-Liquid Partitioning in Advanced Nickel-Base Single-Crystal Superalloys, *Metall Mater Trans A*, 36A, 2761-2773.
[11]. Heckl A., Rettig R., Singer R.F.; 2010, Solidification Characteristics and Segregation Behaviour of Nickel-Base Superalloys in Dependence of Different Rhenium and Ruthenium Contents, *Metall Mater Trans A*, 41A, 202-211.
[12]. Matache G., Stefanescu D. M., Puscasu C., Alexandrescu E.; 2016, Dendritic segregation and arm spacing in directionally solidified CMSX-4 superalloy, *Int J Cast Met Res*, 29(5), 303-316
[13]. Pang H.T., D'Souza N., Dong H., Stone H.J., Rae C.M.F.; 2016, Detailed Analysis of the Solution Heat Treatment of a Third-Generation Single-Crystal Nickel-Based Superalloy CMSX-10K, *Metall Mater Trans A*, 47A, 889-906

CALCULATION OF THE DELAMINATION YIELD INDEX

Mihail SIMA[4], Mihaela Raluca CONDRUZ[4], Cristian STĂNICĂ[4]

ABSTRACT: This paper presents a numerical simulation model of the delamination process of a laminated made up of polimerical composite materials ranforced with carbon fibres. Moreover, a set of experimental tests have been done to check the delamination resistance, and the yield indices have been defined and substantiated by generalizing the Hashin-Fabric criterion and the hypotheses of the resistance theories based on the deformation energy and on the distorting energy of the profile.

KEYWORDS: Hashin-Fabric, Tsai-Wu, yield index, delamination, composites

1. INTRODUCTION

Weight reduction of the aircrafts constitutes one of the main directions of action towards diminishing CO_2, NO_x and other burning gases emissions. For this purpose, the use of carbon fibre laminated composite materials with polymeric matrix represents one of the most frequent solutions to be found in the aircraft industry. One main consequence of the large scale use of composite laminated materials was the analysis of their yielding process. Thus, the conclusion was that delamination represents one of the main causes of the yielding phenomenon of various parts made up of carbon fibre ranforced polimerical composite materials [1-3]. The evaluation of delamination resistance can be achieved by using either the release rate of specific energy, ***Gc***, or the calculus of certain yielding indices that have been substantiated on some experimental results (Tsai-Wu, Hill, Hashin, Puck etc.). A comparative analysis between the Von Mises criterion that applies to metals and the criteria applicable to composites indicate a series of similarities. In the case of metallic materials, the Von Mises criterion is defined by relations (1) and (2):

$$\sigma_{VM} = \sqrt{3[(\sigma_1 - \sigma_2)^2 + (\sigma_2 - \sigma_3)^2 + (\sigma_3 - \sigma_1)^2]} \tag{1}$$

$$\sigma_{VM} = \sqrt{3J_2} \tag{2}$$

where J_2 represents the second order degree invariant of the tensor deviation of the stresses.

Similarly, in order to evaluate the resistance of composite material structures specific concepts have been developed based on the Hill criterion (relation (3)) and the Twai-Wu criterion (relation (4)):

$$F_i = F_{11}\sigma_x^2 + F_{22}\sigma_y^2 + 2F_{12}\sigma_x\sigma_y + F_{66}\tau_{xy}^2 \tag{3}$$

$$F_i = F_1\sigma_x + F_2\sigma_y + F_{11}\sigma_x^2 + F_{22}\sigma_y^2 + 2F_{12}\sigma_x\sigma_y + F_{66}\tau_{xy}^2 \tag{4}$$

2. MATERIALS AND PROCEDURES

This paper introduces a new set of relations for the calculus of certain yielding indices though analogy with those defined on the basis of the Hashin Fabric criterion and substantiated on the basis of the resistance theorie related to the deformation energy and to the profile deforming energy. According to the preliminary hypotheses, delamition is going to be initiated within the interlaminar layer if the yielding index is higher than the limit value 1.

[4] National Research and Development Institute for Gas Turbines COMOTI, Bucharest, Romania

The evaluation of the hypotheses taken into consideration has been achieved though the correlation analysis between the values of the yielding indices previously mentioned and the experimental results. Similar approaches to defining certain yielding indices specific for cantivelver beams made up of composite material laminates renforced with carbon fibres are presented in [4]. The interlaminary layer has been considered to be homogenous, and having the mechanical properties of the polymeric matrix and a thickness of at least 25 times smaller than the carbon fibre layer. The experimental data obtained through the delamination of the DCB test pieces ("double cantivelver beam") have been undergone according to the provisions of the standards in [5, 6].

Fig. 1 The test pieces DCB

The rate of the energy released though the propagation of the split (delamination) in mode I has been calculated by using relation (5):

$$G_I = \frac{3P\delta}{2ba} \tag{5}$$

where ***a*** – the length of the delaminated area; ***b*** – the width of the test piece; ***P*** – the force applied on the jaws; $\boldsymbol{\delta}$ - shifting of the jaws.

In the case of DCB test pieces, considering that the stress is placed within the interlaminar layer, the yield index, defined by analogy with the Hashin-Fabric criterion and based on the theory of deformation energy, is:

$$F_1 = \left(\frac{\sigma_y}{\sigma_t}\right)^2 + 2.6\left(\frac{\tau_{max}}{ILSS}\right)^2 \tag{6}$$

Similarly, the yield index calculated as based on the hypothesis of the profile deforming energy is determined though the following relation:

$$F_1 = \left(\frac{\sigma_y}{\sigma_t}\right)^2 + 3\left(\frac{\tau_{max}}{ILSS}\right)^2 \tag{7}$$

The fact that delamination propagates though the yielding of the interlaminar layer has determined us to use the yield point of torsional shear in the interlaminar layer (ILSS –" interlaminar shear strength") OY oriented, that is perpendicular on the interlaminar layer.

3. ANALYSIS OF THE EXPERIMENTAL DATA

Fig. 2 shows the graphics of the experimental data concerning the variation of force vs displacement of the jaws, Fig. 3 shows the distribution of normal tension in the interface layer, and Table 1 shows the rate of energy release on the extension of delamination.

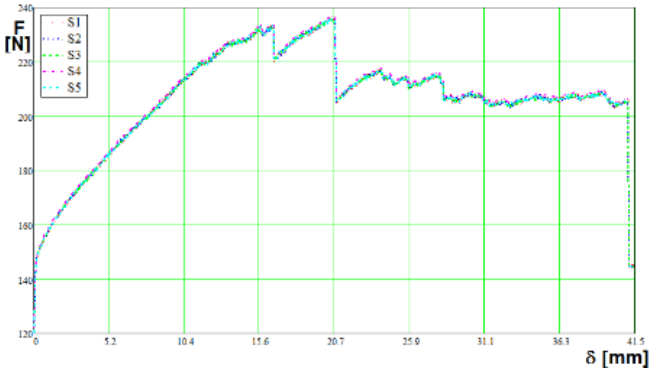

Fig. 2 The variation of force vs displacement of the jaws

Table 1. Critical Extension Force G_c

Displacement [mm]	Force [N]	a [mm]	G_c [N/m]	$\frac{\Delta G_c}{G_c}$	ΔG_c [N/m]
17.07987	224.4145	50	4599.565	3.71%	124.70
20.85475	235.3526	59	4991.41	3.28%	163.68
24.9-41.06525	213.06-206.1	64	4973.617	3.13%	155.64
41.49787	145.544	98	5181.98	2.63%	136.21

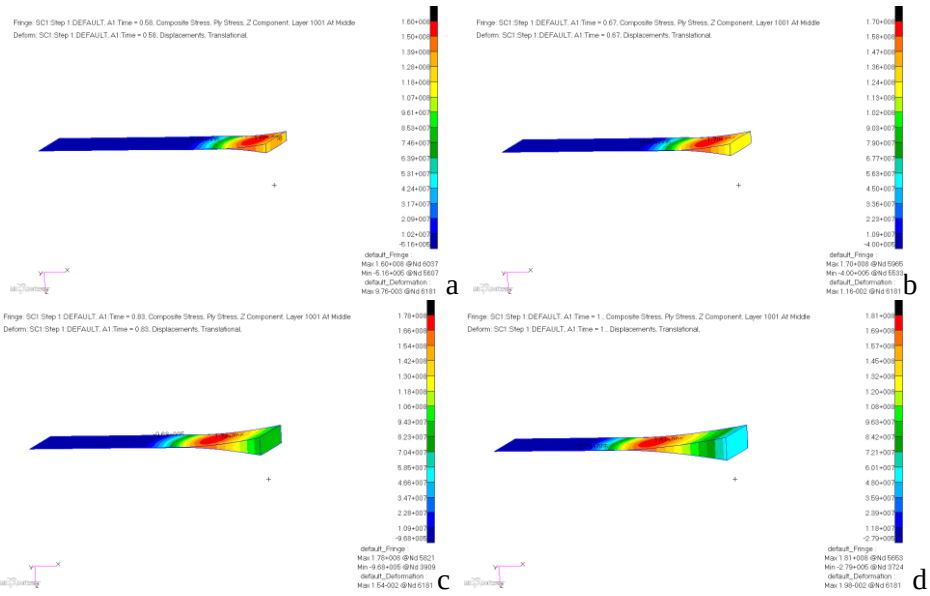

Fig. 3 Distribution of normal tension in the interface layer [Pa]: a) the length of the 50 mm split, b) the length of the 53 mm split, c) the length of the 64 mm split, d) the length of the 98 mm split

Table 2 presents the values of the yield index calculated by means of the Hashin-Fabric criterion and of the yield theories of material resistance based on the hypothesis of the deformation energy, and on the profile deforming energy respectively.

Table 2. Yield indices corresponding to the delamination phases and calculated on the basis of the Hashin-Fabric criterion as well as on the theories of material resistance

a [mm]	σ_z [MPa]	σ_t [MPa]	τ_{max} [MPa]	$ILSS$ [MPa]	$F_1 = \left(\frac{\sigma_y}{\sigma_t}\right)^2 + \left(\frac{\tau_{max}}{ILSS}\right)^2$	$F_1 = \left(\frac{\sigma_y}{\sigma_t}\right)^2 + 3\left(\frac{\tau_{max}}{ILSS}\right)^2$	$F_1 = \left(\frac{\sigma_y}{\sigma_t}\right)^2 + 2.6\left(\frac{\tau_{max}}{ILSS}\right)^2$
50	160	200	21.5	60	0.77	1.03	0.97
53	170	200	21.5	60	0.85	1.11	1.06
64	178	200	21.5	60	0.92	1.18	1.13
93	181	200	21.5	60	0.95	1.20	1.15

Modelling of the interlaminar layer as a homogeneous layer having the mechanic characteristics of the matrix and the use of a yielding criterion, mainly defined according to the hypothesis of the profile deforming energy, ensures consistency between the FEA analysis and the experimental data. The correlation analysis between the yileding index calculated on the basis of the Hashin-Fabric criterion and the experimentally determined yielding indicate lower values of the Hashin-Fabric yielding indices: 0.77-0.95.

The subunitary values of the yielding index are corresponding to the situation in which the material does not deteriorate (delamination is not initiated). Actually, the interlaminar layer is not a homogenous stratum, while the acrbon fibres corresponding to the two transversal directions are not coplanary, their position having a direct impact on the geometry of the interlaminar layer; the interface between these fibres and the interlaminar layer constitute a concentration factor. Thus, the mechanical properties of the interlaminar layer should be adjusted and therefore, the development of this direction of action requires an approach into the micro-mechanic field.

4. CONCLUSIONS

The yield indices substantiated on the hypothesis of the profile deforming energy register supraunitary values, 1.03-1.02, and are consistent with the experimental results. On the analysis of the correlation between the yielding indices calculated according to the deformation energy hypothesis, the only inconsistency is present in the case of the first delamination, when the calculated index is 0.97, while the relative error of calculation of the critical rate of specific energy release is 3.7 %. Considering the correlation analysis results, we may conclude by saying that the proposed model ensures consistency with the experimental data, as long as the yielding criterion substantiated on the basis of the profile deforming energy is being used. In the case of the hypothesis of the deformation energy, there is an inconsistency between the calculated index and the initiation of delamination. The experimental results have been obtained by testing 5 samples (Mode I delamination), and for the validation of these hypotheses further tests will be done by using a larger number of test pieces and by studying delamination in the case of Mode II and Mode III of stress or in the case of a combination of the three modes (complex stress).

ACKNOWLEDGMENTS

This work was carried out within “Nucleu” Program TURBO 2020, supported by the Romanian Minister of Research and Innovation, project number PN 16.26.03.04.

REFERENCES

[1]. Davies G.A.O, Hitchings D., Ankersen J.; 2006; Predicting delamination and debonding in modern aerospace composite structures, Composites Science and Technology, Vol. 66, Issue 6, pp. 846–854
[2]. Lou X., Cai H., Yu P., Jiao F., Han H.; 2017; Failure analysis of composite laminate under low-velocity impact based on micromechanics of failure, Composite Structures, Vol. 163, pp. 238-247
[3]. Yao L., Sun Y., Zhao M., Alderliesten R.C., Benedictus R.; 2017; Stress ratio dependence of fibre bridging significance in mode I fatigue delamination growth of composite laminates, Composites Part A: Applied Science and Manufacturing, Vol. 95, pp. 65-74
[4]. Thurnherr C., Groh R.M.J., Ermanni P., Weaver P.M.; 2017; Investigation of failure initiation in curved compozite laminates using a higher-order beam model., Composite Structures, In Press, Accepted Manuscript
[5]. ASM D 5528-01 – Standard test Method or Mode I Interlaminar Fracture Toughness of Unidirectional Fiber-Reinforced Polymer Matrix Compozites;
[6]. Landry B., LaPlante G., LeBlanc L.R.; 2012; Environmental effects on mode II fatigue delamination growth in an aerospace grade carbon/epoxy compozite, Composites Part A: Applied Science and Manufacturing, Vol. 43, Issue 3, pp. 475–485

CARBON NANOTUBE AND NANOCLAY BASED POLYMERIC COMPOSITES – RECENT ACHIEVEMENTS AND FUTURE DEVELOPMENT DIRECTIONS

Mihaela Raluca CONDRUZ[5], Ionuț Sebastian VINTILĂ[5]

ABSTRACT: A literature survey was conducted to determine the trends in polymer composite field. It is foreseen that the future composite material design will consist in nanocomposites or in hybrid laminates. The purpose of the nanomaterials integration is to improve the current composite's properties, like mechanical properties (tensile strength, interlaminar shear strength, stiffness and impact resistance), thermal and electrical conductivity and electromagnetic interference resistance, to provide structures with superior characteristics compared with the structures curently used.

KEYWORDS: composite materials, carbon nanotubes, nanoclay, buckypaper, hybrid composites

1. INTRODUCTION

The design stage of a new product implies the selection of materials, optimum manufacturing technologies and development of structural material designs that fulfil the imposed requirements. Fibre reinforced polymeric composites are integrated in almost all industrial areas, especially in the aerospace field. They are used due to their high performances and mechanical properties and low density. Improvements were made in the last decades in the material science field due to nanotechnology development. Through integration of nanomaterials in advanced composites can improve their properties without affecting their density and mass.

2. STATE OF THE ART

Carbon materials are widely used in various forms, such as fibres and flakes, as reinforcements and additives to improve properties of polymers. In aviation, the use of carbon fibre composites in 50% of Boeing 787's structural weight is the greatest achievement of composites research over the past 5 decades [1]. In the last two decades, the researches were focused on different types of reinforcing elements for polymeric composites like carbon nanofibers (CNFs), carbon nanotubes (CNTs), graphite nanoplatelets (GNPs) and nanoclay (NC). Nowadays the nanotechnology is one of the most popular areas of research and includes all technical disciplines [2]. The material's nanostructure is a key factor for the development of novel properties [3] because improved interface interactions can lead to enhanced properties of the materials at larger scale. The nanomaterials have an extremely high surface to volume ratio which considerable changes their properties when compared with their bulk sized equivalents [3-5]. Nanocomposite materials have been studied for more than 50 years, the first reference on nanocomposites was made in 1950, and polyamide nanocomposites were reported as early as 1976 [3]. The development of nanotechnology was encouraged by the discovery of carbon nanotubes in the early 1990s [6]. The first CNTs discovered were MWCNTs (multiwall carbon nanotubes), which consist in multiple concentric cylindrical layers of graphene sheets coaxially arranged around a central hollow core. Later, SWCNTs (single wall carbon nanotubes) were produced which consist in a single graphene cylinder [7]. Now the nanocomposite materials are considered the materials of the 21st century due to the combination of their properties and which are not found in conventional materials [4, 5]. Typically, the nanocomposites consist in a combination of clay/carbon and polymers, and this class of nanocomposites is a fast-growing area of research [3].

[5] National Research and Development Institute for Gas Turbines COMOTI, Bucharest, Romania

Almost all types of polymers, such as thermoplastics, thermosets and elastomers have been used to make polymer nanocomposites. The two main classes of nanoreinforcement are carbon nanotubes and layered silicate clays (generally referred as nanoclay) [5].

The most studied category of nanocomposites was nanoclay reinforced plastics because the starting clay materials are easily available and because their intercalation chemistry has been studied for a long time [5], but in the last decades, the CNTs based nanocomposites replaced them. The influence of nanoreinforcement on organic materials is known as "nano-effect" [2]. The nano-effect can be observed only if the nanomaterial is well dispersed in the polymeric matrix (nanoscale dispersion). To achieve this kind of dispersion in polymeric matrices, using nanoclay or CNTs is achieved by functionalizing their surfaces because it is a difference between surfaces energies of polymeric materials and nanoreinforcing materials [8].

CNTs have poor dispensability and the tendency to bundle, and on the other hand, nanoclay have to let the polymeric chains to intercalate their galleries [8,9]. The surface energy of clay layers is lowered by their surface modification with surfactants that have compatibility with the organic polymers, the surfactant expands clay galleries and increase the spacing between the layers (d-spacing) [8].

During the synthesis, the CNTs are contaminated with metallic and amorphous impurities so they have to be further purified. The purifying process enhances the bad dispersion and poor interactions between polymeric matrices and CNTs and they have to be functionalized. The functionalization methods of CNTs can be divided into chemical (covalent) and physical (noncovalent) [10]. Recently, the CNTs based nanocomposites started to replace the fibre reinforced composites in aerospace structural components. The F-35 Lightning II Lockheed Martin wing tip fairings are made of CNTs and epoxy resin [11].

Nanomaterials were used in different studies as additional reinforcing materials for polymeric composite reinforced with fibres, composites based on prepreg precursors. The additional reinforcing agent is added between the prepreg plies to improve the properties of the laminates, especially the mechanical properties.

Quaresimin et. al. [12] studied the interlaminar properties of clay-modified epoxies and their glass reinforced laminates. They observed a significant improvement in the fracture toughness and crack propagation threshold of clay-modified epoxy. However, due to the nanofiller morphology, the behaviour of clay-modified laminates was comparable to that of the base laminates.

Rafiq et. al. [13] studied the impact resistance of hybrid glass fiber reinforced epoxy/nanoclay composite laminates. It was found that the addition of nanoclay improved the peak load, the stiffness and also the physical damage was reduced in case of the laminates integrating 1.5wt% nanoclay. In case of samples with 3.0 wt% the impact resistance wasn't improved due to the clay agglomeration.

Helmy et.al. [14] studied the tensile fatigue behaviour of glass-epoxy tapered beam composites with different stacking sequences, where nanoclay had been incorporated. It was observed that static tensile strength and modulus of glass-epoxy tapered composites were slightly enhanced by the addition of nanoclay and it suppresses the fatigue damage growth in terms of damage index and crack growth rate over the whole fatigue life except the early stage of loading.

Arai et. al. [15] studied the interlaminar fracture toughness mode I and II for carbon fibre-epoxy laminates toughened by a carbon nanofibre interlayer. A paste was made of carbon nanofibres and ethanol and was applied by hand on carbon fiber prepreg sheets using a metal roller. The solvent was evaporated and the prepreg plies were bonded together. Standard DCB (double cantilever beam) and ENF (end notch flexure) specimens were prepared and tested. The tests showed that the hybrid composites showed approximatively 50% increase of model fracture toughness and 2-3 times greater mode II interlaminar fracture toughness than references.

Davis et.al. [16,17] assessed the ability of f-CNTs (fluorine functionalized carbon nanotubes) to improve the interlaminar fracture toughness, tensile strength and stiffness of polymeric composites. They used four-harness satin weave carbon fibre and epoxy resin. The f-CNTs were integrated by solvent spraying method. Four-point ENF tests, tensile tests, tension-tension and tension-compression cycling tests were performed. The results showed that f-CNTs increased the interlaminar fracture toughness by 27% in case of 0.5 wt% f-CNTs compared with the neat composite laminate; the laminate tensile strength was improved up to 18% and 24% in case of the stiffness.

Another method to integrate the CNTs in polymeric composite laminates is using buckypapers (BP). Buckypapers are thin films with paper-like morphology manufactured from self-supporting network of entangled CNTs held together by the van der Waals interactions [18].

Usually, BPs are manufactured by suspension filtering under positive or negative pressure and by frit compression. The common solvents used to disperse the CNTs are ethanol or methanol. Another method used to manufacture BPs is by liberation of electrophoretically deposited carbon nanotubes [19].

Fig. 1 presents a SEM image of a hybrid composite laminate which integrates CNTs between two unidirectional carbon fibre prepreg plies. Fig. 2 presents examples of BPs with different diameters.

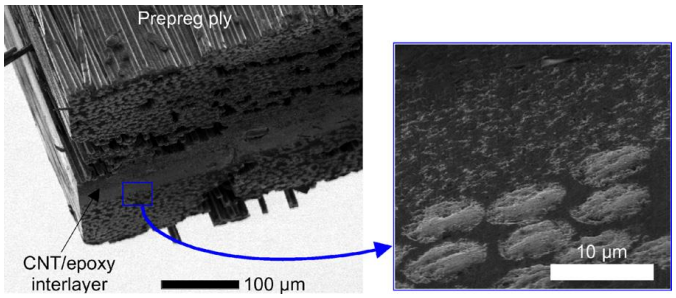

Fig. 1 Hybrid composite laminate realised by the integration of CNTs between two prepreg plies [20]

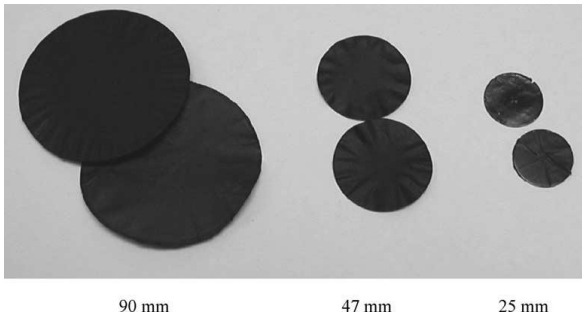

Fig. 2 Buckypapers [21]

3. DISCUSSION

The literature review was conducted to determine the research trends in the polymeric composite field. It was noticed that most of the researches lead to the improvement of common polymeric materials and polymeric composites properties by nanoreinforcement.

Polymeric materials filled with nanomaterials are considered polymeric nanocomposites and by adding nanomaterials to fibre reinforced laminates are manufactured hybrid polymeric composites. The main goal of this types of new materials is to improve the properties of the materials and the overall performance of the structure which is made with those material designs.

The main properties that are currently under study, and which scientists are trying to improve, are the mechanical properties of neat thermoset polymers and common composite laminates, properties like tensile strength, interlaminar fracture tougthness, stiffness and impact resistance.

Several other properties can be improved by the addition of nanomaterials, properties like the electrical and thermal conductivity of polymers and advanced composites, thermal and dimensional stability (by increasing the glass transition temperature – Tg of polymers, which influence the thermal resistance of the polymer), flame retardant properties, radiation shielding, electromagnetic interference resistance and lightning strike protection.

In future work, several structural composite material designs consisting in nanocomposites and hybrid laminates will be manufactured and tested to evaluate their properties improvement compared with current advanced composite properties. The properties of material designs will be studied and optimized along with the nano-effect of the nanoreinforcement on neat epoxy and prepregs (nano-effect on Tg and viscosity of the neat epoxy, on mechanical properties like tensile strength and elastic modulus, drop weight impact resistance, flexural strength, interlaminar fracture toughness). The suitability of the materials for aerospace applications will be evaluated.

4. CONCLUSIONS

Based on their outstanding properties, in the future decades polymeric nanocomposites can replace the current fibre reinforced composites for particular applications. All industrial sectors can benefit of the weight reduction (compared with the fibre reinforced composite's weight), enhanced properties and tailorability of nanocomposites.

ACKNOWLEDGEMENT

This work was carried out within "Nucleu" Program TURBO 2020, supported by the Romanian Minister of Research and Innovation, project number PN 16.26.04.04.

REFERENCES

[1] Hahn H.T., Choi O.; 2011, Graphite Nanoplatelet Composites and Their Applications, Ed. Nicolais L., Meo M., Milella E., *Composite Materials: A Vision for the Future*, Springer, 169-186
[2] Paul D.R., Robeson L.M.; 2008, Polymer nanotechnology: Nanocomposites; *Polymer Journal*, 49, 3187-3204
[3] Okpala C.C.; 2013, Nanocomposites – An Overview, *International Journal of Engineering Research and Development*, 8, 17-23
[4] Camargo P.H.C., Satyanarayana K.G., Wypych F., 2009, Nanocomposites: Synthesis, Structure, Properties and New Application Opportunities, *Materials Research*, 12, 1-39
[5] Anandhan S., Bandyopadhyay S., 2011, Polymer Nanocomposites: From Synthesis to Applications; Ed. Cuppoletti J., *Nanocomposites and Polymers with Analytical Methods*; InTech, 3-28
[6] Iijima S.; 1991, Helical microtubes of graphitic carbon, *Nature*, 354, 56-58
[7] Schadler L.S.; 2003, Polymer-based and Polymer-filled Nanocomposites; Ed. Ajayan P.M., Schadler L.S., Braun P.V; *Nanocomposite Science and Technology*; WILEY-VCH Verlag GmbH Co. KGaA; Weinheim; 77-154
[8] Nazid M.S., Kassim M.H.M., Mohapatra L., Gilani M.A., Raza M.R., Majeed K.; 2016, Nanocomposites, Nanoclay Reinforced Polymer Composites;Ed. Jawaid M., Qaiss A.e.K, Bouhfid R., *Nanocomposites and Bionanocomposites*; Springer, XII, 35-55
[9] Ahmed D.S, Haider A.J., Mohammad M.R; 2013, Comparesion of Functionalization of multi-walled carbon nanotubes treated by oil olive and nitric acid and their characterization; *Energy Procedia*; 36; 1111-1118
[10] Jeon I.Y., Chang D.W., Kumar N.A., Baek J.B; 2011, Functionalization of Carbon Nanotubes, Carbon Nanotubes, Ed. Yellampalli S., *Carbon Nanotubes - Polymer Nanocomposites*, InTech, 91-110
[11] Gay D.; 2015, *Composite Materials Design and Applications*,Third Edition; CRC Press, 62
[12] Quaresimin M., Salviato M., Zappalorto M.; 2012, Fracture and interlaminar properties of clay-modified epoxies and their glass reinforced laminates, *Engineering Fracture Mechanics*, 81, 80-93
[13] Rafiq A., Merah N., Boukhili E., Al-Qadhi M.; 2017, Impact resistance of hybrid glass fiber reinforced epoxy/nanoclay composite; *Polymer Testing*, 57, 1-11
[14] Helmy S., Hoa S.V.; 2014, Tensile fatigue behavior of tapered glass fiber reinforced epoxy composites containing nanoclay, *Composites Science and Technology*, 102, 10-19
[15] Arai M., Noro Y., Koh-ichi S., Endo M.; 2008, Mode I and mode II interlaminar fracture toughness of CFRP laminates toughened by carbon nanofiber interlayer, *Composites Science and Technology*, 68, 516-525
[16] Davis D., Whelan B.; 2011, An experimental study of interlaminar shear fracture toughness of a nanotube reinforced composite, *Composites: Part B*, 42, 105-116
[17] Davis D., Wilkerson J., Zhu J., Ayewah D.;2010, Improvement in mechanical properties of a carbon fiber epoxy composite using nanotube science and technology, *Composite Structures*, 92, 2653-2662
[18] Wan Dalina W.A.D, Tan S.H., Mariatti M.; 2016, Properties of Fiberglass/MWCNTS Buckypaper/Epoxy Laminated Composites, *Procedia Chemistry*, 19, 935-942
[19] Wang X., Lu S., Ma K., Xiong X., Zhang H., Xu M.; 2015, Tensile strain sensing of buckypaper and buckypaper composites, *Materials and Design*, 88, 414-419
[20] Garcia E.J., Wardle B., Hart A.J.; 2008, Joining prepreg composite interfaces with aligned carbon nanotubes, *Composites: Part A*, 39, 1065-1070
[21] Wang Z., Liang Z., Wang B., Zhang C., Kramer L.; 2004, Processing and property investigation of single-walled carbon nanotube (SWNT) buckypaper/epoxy resin matrix nanocomposites, *Composites: Part A*, 35, 1225-1232

LUBRICATION OPTIMIZATION OF A SCREW COMPRESSOR USED FOR NATURAL GAS

Victoria TELEABA[6], Mihaiella CREȚU[6], Radu MIREA[6]

ABSTRACT: Present paper shows the lab tests results for oil samples obtained during the monitoring process within period 12.2016 – 01.2017 from compressor C4 deployed at Munteni extraction site, which uses PAG oil. Base characteristics determinations were performed as well as FTIR testing for the samples tapped at 3171 and 3195 working hours before and after the periodical maintenance of the compressor, when 60 more liters of new oil have been added. The degradation tendency of the oil was assessed. The preliminary conclusions regarding the degradation of base characteristics, emphasizes a better maintenance of these characteristics related to the previous used oil. The degradation tendency of the oil is currently under analysis and also it's compatibility with polymeric parts of the compressor is assessed.

KEYWORDS: screw compressor, degradation, oil, poly-alpha-olephn, poly-alkylen-glycol, FTIR

NOMENCLATURE
PAO – poly-alpha-olephin
PAG – poly-alkylen-glycol
IR – infrared
FTIR – mass spectroscopy infrared with Fourier transform

1. INTRODUCTION

A continuous a periodical analysis of the used oils for screw compressors is made by COMOTI since the maintenance task falls into its task. Also, testing new oil based on specially designed compounds that enhances the functionality and life span of the compressors is currently undergoing. The final aim is to be able to formulate and select the specific type of oil best fitting the specific application. The aim of the paper is to test within the laboratory oil samples obtained during the monitoring process of a screw compressor. The chosen one is C4 compressor deployed at Munteni extraction site. This compressor initially used a PAO based oil, but, considering its degradation tendency, mainly related to its base characteristics, the replacement of the oil was performed. The new oil is a PAG based oil and its degradation tendency in terms of base characteristics was assessed. The tests and results showed within the current paper were made after 3171 and 3192 working hours, before and after the periodical maintenance of the compressor when 60 litters of new oil have been added. The results have been compared with the ones obtained on the unused oil and also with the ones obtained on PAO oil used before it. Aside from the testing of the behaviour of oil's base characteristics, a FTIR analysis was performed in order to assess the degradation of the oil from chemical point of view during its exploitation. Also, the behaviour of the equipment running on PAG oil was assessed before 3195 working hours and before and after periodical maintenance.

What is specific worldwide for the operation of a screw compressor is that oil is continuously injected into the compressor, both to cool the gas during compression and to lubricate and cool the compressor's parts, while the most important characteristics required for oil are viscosity, density, flash point, foaming characteristics and acid number [1]. Any lubricant/ oil contains the so-called "base oil" (75-85% of the end product) and a set of additives (15-25%) used to enhance the performance of the base oil and to eliminate adverse properties that can be generated during exploitation [2]. There are two main types of base oils: mineral and synthetic. Mineral base oil is derived from the purification of crude oil, whereas the synthetic on is a chemical obtained from contaminant - free pure compounds intended for lubrication tasks.

[6] National Research and Development Institute for Gas Turbines COMOTI, Bucharest, Romania

The main component of synthetic base oil is "designed" as a product of a chemical reaction between two or more substances, depending on the desired performance in a specific application, which makes up the major advantage of synthetic lubricants. Their advantages also include resistance to oxidation and high temperature, very good mechanical strength, very good adhesion to lubricated surfaces, all ultimately resulting in significantly higher energy efficiency. In order to keep a rigorous eye on the operation of the industrial plants, specific sampling strategies are in place (points along critical routes) and regular specific tests are performed [3], [4].

The matter of developing a specific type of oil for natural gas compression equipment, in Romania, has not been seriously addressed so far, being used only mineral base oils or synthetic PAO base oils having as components that degrade at the same rate. The explanation resides in the natural gas solubility in PAO based mineral oils and synthetic oils compared to other diester and PAG based synthetic oils. The gas dissolved in PAO based mineral and synthetic oils has a constantly decreasing viscosity and flash point, because it contains molecules similar in structure, mainly C-H bonds, unlike diester and PAG based synthetic oils, which are polar molecules. In a PAG molecule, every third atom of the polymer chain is an oxygen atom, which gives its strong polarity, therefore, the hydrocarbons in gas are practically insoluble in PAG.

2. PROCEDURES

2.1. Determination of base characteristics of the obtained samples

BASF PLURASAFE CL GAS 9 is PAG based oil developed by German producer BASF and it is tested for the first time in Romania on a natural gas screw compressor. The chosen compressor is C4 which is deployed in Munteni extraction site. The main purpose of its use is to formulate and establish an optimal composition for oil especially designed for this location. The oil's formula is an experimental one developed by BASF having the technical characteristics presented in [5]. The paper presents sampling tests made for 3171 – 3195 working hours on oil's base characteristics. The samples were clear but with different colours (light orange to light green) compared with the samples kept within the laboratory and having a small superior layer, clear and darker, non-miscible with the product, having small mechanical impurities - sample 3171h. As the sample rests, its colour gradually turned orange as the unused oil and other samples, as seen in Fig. 1.

Samples at 4 days	Samples at 5 days	Samples at 11 days	Samples at 14 days	Samples at 52 days

Fig. 1 BASF PLURASAFE CL GAS 9 at 3171 and 3195 working hours

The obtained values for the viscosity at 40^0C and flash point emphasises a 10-12% decrease for viscosity and 42-45% for flash point compared with the new, unused sample as seen in Table 1. The obtained results for viscosity are similar with the ones obtained by BASF in its own lab.

Tabel 1: Obtained values for PLURASAFE CL GAS 9 at 3171-3195 h

Determined characteristic / Sample	***Viscosity at 40 °C, [mm²/s]***	***Flash point, [C]***
Method	*SR ISO 3104-2002*	*ASTM D92 - 05a*
Equipment	*SCAVINI equipment Ubbelohde COMECTA*	*SCAVINI equipment*
Values according to technical sheet BASF TI/EVO 0010 e / Nov. 2015	**105**	**>290**
3171 h	87,8	157,3
3195 h	91,7	168,8

These values obtained for the base characteristics are much higher compared with the ones obtained for PAO oil STABIO S100, also produced by BASF and which was previously used within C4 screw compressor and which shows a decrease of 75% for viscosity and 85% for flash point.

2.2. FTIR tests of the obtained samples

Fourier transform infrared (FTIR) spectroscopy is a versatile tool used to detect common contaminants, lube degradation byproducts and additives within lubricating oils. It has become a widely-used technique for quickly assessing multiple lubricant characteristics. This test method is relatively quick to perform and is capable of simultaneously detecting multiple parameters, including antioxidants, water, soot, fuel, glycol, oil oxidation and certain additives. Adding to the power of this qualitative measurement, the size of the peaks is a direct indication of the amount of the specific material found in the sample. Since most used oil samples are complex mixtures of thousands of different molecules, including base oil molecules, additives, oil degradation byproducts, wear debris and contaminants, the infrared spectrum of the sample is typically complex and can be difficult to interpret with any degree of certainty, as some wavenumbers may overlap. Despite these drawbacks, FTIR still has great value in used oil analysis and is employed by the majority of oil analysis labs as a screening tool [6].

The tests have been performed within Physical-Chemical Determination lab on a FTIR Spectrum Oil Express Series 100, v 3.0 spectrometer provided by Perkin Elmer which has an auto sampler (Fig. 2). The equipment is specially designed for FTIR analysis of used oils, made of: sample purge compartment, optical system in spectral domain 7800-370 cm^{-1} having a resolution of 0.5 cm^{-1}, intermediary IR detector, electronic system with signal processor Motorola DSP56303 and Motorola 68340, PC, Spectrum Software, auto sampler. The used solvent is heptanes.

Fig. 2 Spectrum Oil Express Series 100, v 3.0

As is shown in Table 2, after analyzing the specters, it can be observed that there are no major differences between tested samples. After analyzing the quantitative results, it can be observed the water content decreases as well as OH groups. There are no traces of oxidation normally present in synthetic oils as SO^4 groups and also there are no traces of gasoline. Both samples, 3171 and 3195 h were collected after the gasoline layer has been drained. This is the best argument that PAG is not compatible with gasoline, therefore the gasoline does not mix with it.

Table 2. FTIR results for PLURASAFE CL GAS 9 at 3171-3195 h

Reference	3171 h	3195 h
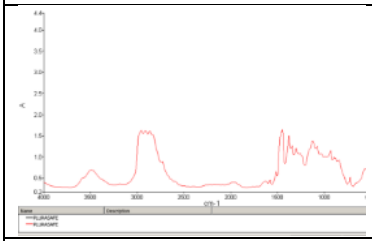	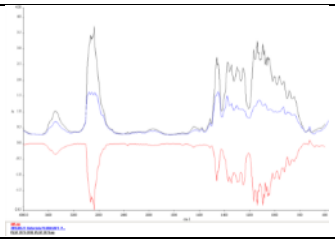	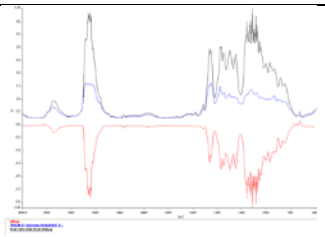
Differences from reference:	- acidic/aminic salts (2650-2385) - compounds with H links (2650-2350, 0900-0650) - water (3650-3150)	- hydroxi groups (3650-3595) - metallic oxydes (0800-0705) - water (3650-3150)

PLURASAFE CL Gas 9 is PAG based oil having exceptional anti ware properties. Thus, that kind of base oils need less anti ware additives as PAO or mineral based oils. These anti ware additives are a particular formulation from BASF.

Relevant indicators for these industrial lubricants are viscosity and iron content. For PLURASAFE CL Gas 9, viscosity tests have been performed both by COMOTI and BASF labs and iron content tests have been performed only by BASF. Related to viscosity tests, the results are similar from COMOTI and BASF labs. Related to iron content tests, the results show less than 5ppm (value that is very close to the detection limit), compared with PAO based oil STABIO S100 which had 19 ppm.

3. CONCLUSIONS

From base characteristics point of view (viscosity and flash point), PAG based PLURASAFE CL GAS 9 oil presents superior values comparing with PAO based STABIO S100, due to its incopatibility with the gasolines. The main reason is that it's molecules show an increased polarity realted to PAO based oil. This tendency was present from the begining and continued since 3195 working hours.

PAG based PLURASAFE CL GAS 9 oil presents H_2O and OH traces comapring with PAO based STABIO S100. This is due to the compatibility of its molecular inner structure with water.

PAG based PLURASAFE CL GAS 9 oil show a better anti ware characteristic. Iron content is 5ppm comapred with 19 ppm for PAO based STABIO S100.

PAG based PLURASAFE CL GAS 9 oil shows no traces of oxidation which are normally present in synthetic oils as SO^4 groups and also there are no traces of gasoline.

AKNOWLEDGEMENTS

This work was carried out within "Nucleu" Program TURBO 2020, supported by the Romanian Minister of Research and Innovation, project number PN 16.26.06.06.

4. REFERENCES

[1] Ed. Dowson D.; 1993, Physical Properties of Lubricants, Engineering Tribology, Tribology Series Vol. 24, 11–57
[2] Componenta lubrifiantilor, http://www.xoil.ro/lubrifianti/tribologie/
[3]Vidrighin C.; 2013, "Strategii pentru evaluarea analitică a lubrifianţilor industriali", http://www.ttonline.ro/autori/costin-vidrighin
[4] Vidrighin C.; 2013, "Programe de analiza a lubrifiantilor", http://www.ttonline.ro/autori/costin-vidrighin
[5] http://www.ilco-chemie.de/downloads/Plurasafe_CL_Gas_9.pdf
[6] Wright J.; 2015,"Benefits of FTIR oil analysis", Machinery lubrication, no. 8

PRELIMINARY RESULTS REGARDING THE SOLUTION FOR A GASEOUS-LIQUID BURNER

Ene BARBU[7], Andreea MANGRA[7]

ABSTRACT: Fuel flexibility is a fundamental attribute of combustion installations that equip turboengines and heat recovery steam generators of cogenerative groups. Therefore, the main objective of the PN 16.26.01.08 project was the study the thermogasodynamic processes in an afterburner and its interaction with the turboengine, in order to develop a modern technology of design, manufacturing and testing facilities of multifuel, gaseous-liquid, afterburner. Research focused on the development of a mono-modular natural gas / kerosene afterburner, with the possibility to function with natural gas / biofuel obtained from camelina. This paper presents preliminary results regarding defining the gaseous-liquid afterburner solution, through numerical modeling, based on the experience gained by National Research and Development Institute for Gas Turbines COMOTI in the field of turboengines and their exploitation, particularly regarding the 2xST 18 Powerplant from Suplacu de Barcau.The gaseous-liquid afterburner optimal solution will be selected after completing the numerical simulations and corresponding tests.

KEYWORDS: burner, afterburner, natural gas, kerosene, camelina

NOMENCLATURE

P_t–thermic power of the burner [kW];
t_{ma}–upstream maximum temperature [^{0}C];
t_{mv}–downstream maximum temperature [^{0}C];

1. INTRODUCTION

The basic fuel for the operation of gas turbine cogeneration groups is natural gas, but the requirements to conserve the fossil fuel reserves and protect the environment have led to reorientation towards alternative fuel sources.

The afterburner installation can function with a much wider range of fuels than those accepted by the gasturbine, which leads to an increase of the cogenerative group fuel flexibility.

EU's Directive 2003/30/CE aim is promoting the use of biofuels and other renewable fuels, especially in the transport sector, thus reducing the dependence of energy and lowering the greenhouse gases emissions. Already Airbus and TAROM, with a consortium of partners, have established one of the first projects at European level aiming to develop an aviation biofuel (biokerosene) production and processing unit. In comparison with other crops, camelina is resistant to drought and cold, does not require large investments, can be grown in successive crops, thus making it attractive for biofuel production [1].

Because it is not widely used in nutrition, it also has the advantage of not jeopardizing food supplies of the population. In comparison with other oleaginous plant, the camelina seeds have an over 35% oil content [2]. Biokerosene has been obtained from camelina oil, by hydrotreatment.

However, at the moment the production of biokerosene is expensive, sophisticated processing technology being required. Under these conditions, it has been raised the question regarding the possibility of using camelina oil as fuel or additive to a fuel in transport or energetic field [2].

[7]National Research and Development Institute for Gas Turbines COMOTI, Bucharest, Romania

2. RESEARCH, TECHNICAL-SCIENTIFIC SOLUTIONS

This paper presents preliminary results regarding the study of a gaseous-liquid burner solution, using as fuel natural gas/kerosene or natural gas/camelina oil, obtained within PN 16.26.01.08 project. The project aims to study the thermogasodynamic processes in an afterburner installation and its interaction with the gas turbine, in order to develop a modern technology of design, manufacturing and testing facilities for a multifuel gaseous-liquid afterburner.

Worldwide there are companies that produce gaseous-liquid afterburner installations (Pillard, Coen, Hamworthy Combustion etc.). From the available data, there is no information regarding research related to the use of camelina oil as fuel on an afterburner installation. The interaction of the jets is still a problem to be studied [3, 4]. Insufficient knowledge of these phenomena leads to the increase of NOx emissions and/or flashback.

The elaboration of the gaseous-liquid afterburner constructive solution was based on:the afterburner installation, operating with gaseous fuel, installed at the 2xST 18 Powerplant from Suplacu de Barcau and the experiments carried on an equivalent of that burner, with 3 modules(Fig. 1 left); tests on a single module afterburner operating with natural gas and air (Fig. 2), carried out at the Department of boilers and steam and gas turbines from UPB [5, 6]. Given the trends around the world regarding the modular design, the gaseous-liquid burner study solution followed this direction. The design data, for a single afterburner module, is given in Table 1. Bearing in mind the need to study the interaction of fuel jets, there have been considered 2 burner geometries on which were performed numerical simulations of the combustion process, using ANSYS CFX.

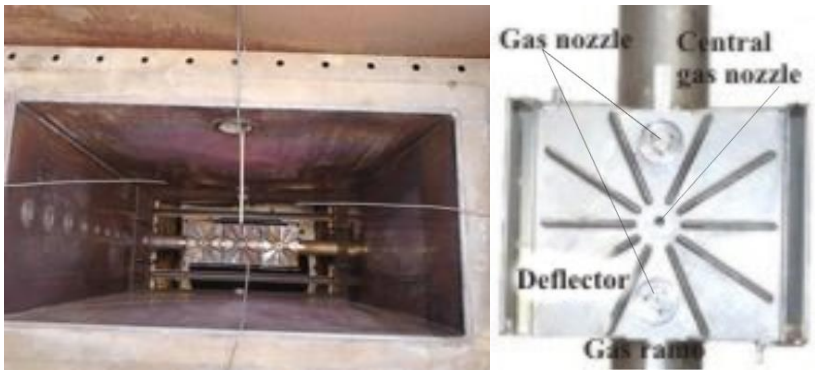

Fig. 1 The 2xST 18 Powerplant afterburner equivalent, on natural gas, mounted on the test bench at INCDT COMOTI (left) and afterburner module structure (right) [5, 7]

Fig. 2 Single module afterburner (left), tested on natural gas with air at UPB (right)

Corresponding to the burner in Fig. 1, the v.1 gaseous-liquid burner geometry version has resulted as follows: the deflector of the central module and its gaseous fuel nozzles have been eliminated, in their place a Delavan type [8] liquid fuel nozzle has been introduced; the other 2 lateral modules and their gaseous fuel nozzles remaining unchanged (the design of the 2xST 18 Powerplant afterburner fuel nozzles has been kept).

The v.2 geometry version is similar to version v.1. The liquid fuel nozzle has been kept. In addition, it has been inserted the central module deflector with unmodified gaseous fuel nozzles.

Corresponding to the burner in Fig. 2 the geometry version v.3 has been considered. Thus, it will be possible to test a single module afterburner, with the same centred liquid fuel nozzle as in versions v.1 and v.2, but the gaseous fuel nozzles, corresponding to the afterburner module in Fig.1, will be modified.

Table 1. Design data for a single afterburner module, from a gaseous-liquid burner

No.	Parameter	unit	Value
1	Fuel	-	Natural gas / kerosene Natural gas / camelina oil
2	Maximum thermic power [P_t]	kW	400
3	Upstream maximum temperature [t_{ma}]	$^{\circ}$C	550
4	Downstream maximum temperature [t_{mv}]	$^{\circ}$C	1000

3. RESULTS, DISCUSIONS

Basically, the methodology of transition from burning a gaseous fuel to the gaseous-liquid fuel burner through numerical modelling is done in several phases [9]: modelling of the burner using gaseous fuel; modelling using liquid fuel; comparison with design data. After these steps will follow design, manufacturing of the prototype, test etc. In the first phase, CFD modelling of v.1 geometry version was performed, using gaseous fuel for the two side modules, the central liquid fuel nozzle being considered plugged.

Fig. 3 (left) shows the temperature distribution corresponding to the two afterburner modules, using a gas flow rate (modelled as CH_4) of 0.014 kg/s. The higher temperatures are within the afterburner chamber. At the checkpoint, centrally located at a height of 2000 mm from the burner, a temperature of 746 ^{0}C has been obtained, compared to 770 ^{0}C, as it has been taken into account.

In the case of CFD modelling, of the v.1 geometry version, using gaseous fuel,the error is less than 5% and interaction between the main jets of the two modules was not observed (internal recirculation, flashback etc.).

Preliminary results, in the case of this geometry version, indicate the possibility of reducing the error under 1% for the combustion of natural gas with air / exhaust gases from the gas turbine, through appropriate adjustment of the oxidizer flow rate.

In the second phase, there were performed CFD numerical simulations on the v.1 geometry version using liquid fuel, the gaseous fuel nozzles have been considered blocked and the central module deflector removed.

Overall, through its structure, the fuel injector ensures a certain spraying angle to the fuel jet (usually between 30^0-90^0 [7]) and a degree of swirl.

In order to simplify the numerical model, in the first stage of modelling kerosene / air combustion, there was not imposed a spraying angle for the fuel jet. The fuel jet enters on axial direction in the computational domain. In this case the flame significantly stretches, emerging from the afterburner chamber (Fig. 3 right).

In the second geometry version, the reintroduction of the central deflector, in the case of kerosene / air combustion, brings the core of high temperature closer to the burner (Fig. 4 left). But, as observed in the previous case, the flame stretches and emerges from the combustion chamber. Preliminary results of kerosene / air combustion show, in the case of this geometry version, that by imposing a spraying angel of 110^0, for a fuel mass flow rate of 0.008 kg/s, the flame fills all the combustion chamber (Fig. 4 right).

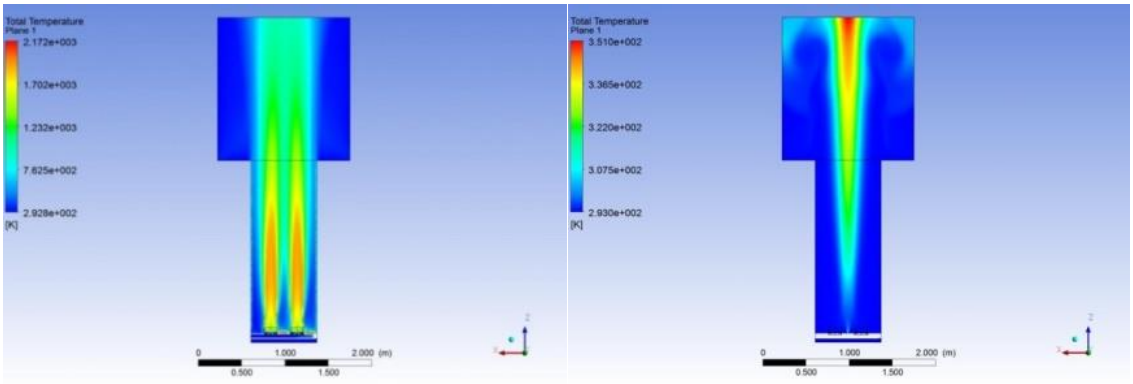

Fig. 3 Temperature distribution for v.1 geometry version without the central deflector, for natural gas/air (left) and for kerosene/air (right)

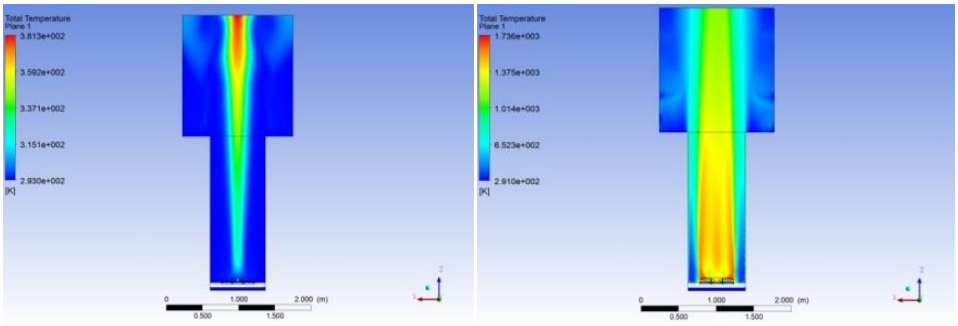

Fig. 4 Temperature distribution for the v.2 burner geometry version, with central deflector, for kerosene/air (left–without spraying angle; right -spraying angle of 110^0)

4. CONCLUSION

Based on the experience gained with the afterburner installation at the 2xST 18 Powerplant, there have been developed 3 gaseous-liquid fuel burner geometry versions, using as fuel natural gas / kerosene or natural gas/ camelina oil.

The numerical modelling is advanced for the version of functioning with natural gas with air / exhaust gases from the gas turbine. The aim is to obtain an error under 1%, for the temperature at the afterburner chamber exit, in the checkpoint located at a height of 2000mm from the burner.

The numerical model for kerosene combustion, with air or gas turbine exhaust gases, has to be improved by adjusting the following data: spraying angle, swirl degree, fuel/oxidizer ratio.

The numerical model for camelina oil combustion, with air/ gas turbine exhaust gases has not yet been approached. The selection of the optimal functioning version for the gaseous-liquid burner will be made after finishing all numerical simulations and validating the results with experimental data.

ACKNOWLEDGMENT

This work was carried out within “Nucleu” Program TURBO 2020, supported by the Romanian Minister of Research and Innovation, project number PN 16.26.01.08.

REFERENCES

[1]. Tenea G. ş. a., 2016, Biocarburant din camelină, Editura Terra Mileniul III, Bucureşti
[2]. Petcu (Mangra) A., 2016, Cercetări privind utilizarea uleiului vegetal de camelină drept combustibil, Teza doctorat UPB, Bucureşti
[3]. Batshon A., Backlund J., Alternate fuels for supplementary firing add value and flexibility to combined cycle and cogeneration plants, http://www.coen.com/library/technical-papers/alternate-fuels-for-supplementary-firing-add-value-and-flexibility-to-combined-cycle-and-cogeneration-plants/
[4]. Burner Qualifications and Capabilities, Zeeco, http://www.errandenterprises.com/zeeco/Burners1.pdf
[5]. Barbu E. et al, 2011, Afterburning Installation Integration into a Cogeneration Power Plant with Gas Turbine by Numerical and Experimental Analysis, Advances in Gas Turbine Technology, Dr. Ernesto Benini (Ed.), ISBN: 978-953-307-611-9, InTech, Croația
[6]. Popescu J. et al, 2010, Researches concerning kerosene-to-landfill gas conversion for an aero-derivative gas turbine, Proceedings of ASME Turbo Expo 2010: Power for Land, Sea and Air, 639-648
[7]. Supplemental firing for cogeneration and combined cycle installation, Bulletin 165C 11/01, http://www.accutherm.com.au/pdfs/accutherm-eclipse-fluefire-burner-013042985804.pdf
[8]. A total look at oil burner nozzles, http://www.delavaninc.com/pdf/total_look.pdf
[9]. Raei B., Abbaspour D., Shahraki F., 2013, Feasibility Study on the Change of Fuel System and Dual-Fuel Burners in Oil Refinery Furnace World Applied Programming, Vol (3), No (6), 212-218

MANAGEMENT SYSTEM FOR POWER PRODUCED BY THE 37 KW EXPANDER-GENERATOR GROUP

Valentin PETRESCU[8], Niculae TOMA[8]

ABSTRACT: National Research & Development Institute for Gas Turbines - Comoti has developed a helical expander - asynchronous electric generator assembly – as well as a test system by tracking the parameters of thermal, mechanical and electrical processes during common or transitory working regimes, their adjustment and control in order to ensure maximum security working conditions. The power supplied by the generator being debited in the COMOTI network. The element of novelty of this electric energy providing assembly constitutes the use of a helical turbine that works at lower speed than other classical expanders due to the elimination of the reductor which ensures the connection of the expander to the electric generator. The monitoring system introduces functional check-ups of the manual and electrical operated elements as well as the check-up of measuring lines of the analog parameters. The testing was done in the testing stand at COMOTI premises and it used air as a working agent. The results thus obtained constitute the preliminary data that may offer the possibility of placing the screw expander - electric generator assembly inside the control and measuring gas stations**.**

KEYWORDS: energetic efficiency, clean energy, helical expander.

1. INTRODUCTION

The applications of the turboexpander in the natural gas industry started about 40 years ago with a small assembly in the south-west of Texas where dr. Judson S. Swearingen attached the first turboexpander for natural gas. Compared to this reference date, the turboexpander technology has developed considerably lately [1]. For example:

- Advances made in dynamics theory and fluid measurement have made it possible to design turboexpanders with high isentropic efficiency and predictive performance;
- The progress in the evaluation of rotor dynamics and of modern analysis of finite elements have led to a better reliability of turbomachinery;
- The increased demand as well as ever higher requests of energy saving have determined the development of more and more large installations.

The year 1980 is a worldwide reference date concerning the use of turboexpanders as facilities for saving the potential energy of high pressure natural gases, which is currently wasted during the process of pressure adjustment and of its transformation into electricity. The use of turboexpanders today represents the most advanced technology used in the electricity production.

The helical expander - asynchronous electric generator assembly is a viable economical solution for retrieving the gas expansion energy in the pressure reduction stations. In order to reduce the pressure of natural gas in the control and measuring stations (SRM) on the main pipelines, rolled valves, heated, are used to reduce the pressure from the transport pressure to the distribution pressure. INCDT-COMOTI has developed an efficient equipment for the conversion of the energy of natural gas expansion into green electricity. This unique group works using oil injection helical technology, which has long been used for screw compressors.

Advantages:

- High efficiency of the product due to the almost isothermal expansion evolution – through warm oil injection;
- Great flexibility with the variations of the gas parameters at the expander imput;
- Minimal foundation due to the permanent rotation movement and to dynamic ballance of the rotors;
- Low maintenance costs due to a very good reliability, few mobile parts (constructive simplicity).

[8] National Research and Development Institute for Gas Turbines COMOTI, Bucharest, Romania

2. MAIN PART

2.1 Paper scope

The proposed solution contains the expander as a source for driving an asynchronous generator over synchronicity. The amount of charged energy is ensured by manually adjusting the gas flow injected into the expander to obtain the nominal slip obtained at the nominal rated current.

The command adjustment and control system for the expander - asynchronous generator group for the tests run at INCDT COMOTI is based on a simple solution considering that the maximum electrical power that the expander-generator assembly can generate can be determined.

The gas controls are mostly manually operated, providing only automatic oil pressure (Pui) control via the oil pump motor drive controller [2].

The helical expander - asynchronous generator group has a test system which monitors the parameters of the thermal, mechanical and electrical processes during normal or transient working regimes, their adjustment and control, in order to achieve a maximum safe operation, the power supplied by the generator being debited in the COMOTI grid.

The monitoring system will require functional checks with manual, electrically driven and linear-level measurement of analogue parameters [3].

2.2 The analysis of the experimental results during nominal or transitory regimes

The start is accomplished by bringing the generator to synchronization speed by the helical expander, followed by the connection to the grid and compared with the synchronous machine it is not necessary to consider the phase position (no special measures are required to connect it to the grid

Completing the electrical connection of the asynchronous generator with a speed deviation of 10% has a negligible influence on the electrical connection. After connecting the asynchronous generator to the grid, the new rotor speed value is set aperiodically, being determined by the ratio between the drive and generator moments. Thus, the fluctuations of active energy felt by the power grid become negligible.

The acquisition of all parameters is done by a computer equipped with a data acquisition board. In the particular case of the used/produced power, a certain „device" or network analyzer takes the values of the currents and voltages for each phase, it calculates and displays several electrical parameters, the active power being one of them. The latter is sent to the data acquisition board under the form of a 4-20 mA unified signal that reflects this power by means of a proportionality ratio. The computer reads this signal, it transforms it into kW, it displays it and saves it on the HDD.

By means of the adjustment of command and control system the following actions are being done:

- testing of the execution elements;
- starting of the expander-generator assembly;
- surveillance of the functioning of the expander-generator assembly during the normal operation regimes;
- communication with the operator;
- disconnection of the expander-generator assembly on the operator's request or automatically due to technological problems.

The graphic representation has had in view 5 decisive parameters for reaching the power performances of the expander - asynchronous generator group:

- PGA (bar), gas pressure;
- P (kW), active power delivered by the generator;
- N (rpm), generator speed.

Maximum power performances are achieved for the constant regime of PGA of about 15 bars (blue color), the value of the transferred power P being of about 36 kW.

In the case of the engine regime, P is placed above the abscissa, while for the generator regime it is placed under the abscissa, and the speed for this regime is of about 3100 rpm

The PGA variations from 0 to 15 bars determine distinct regimes for the electric machine, that is a variation between the engine regime and the generator one, the speed of the generator (N) balancing between 3000 rpm, for the engine regime, and between 3000 - 3100 rpm, in the case of the generator regime.

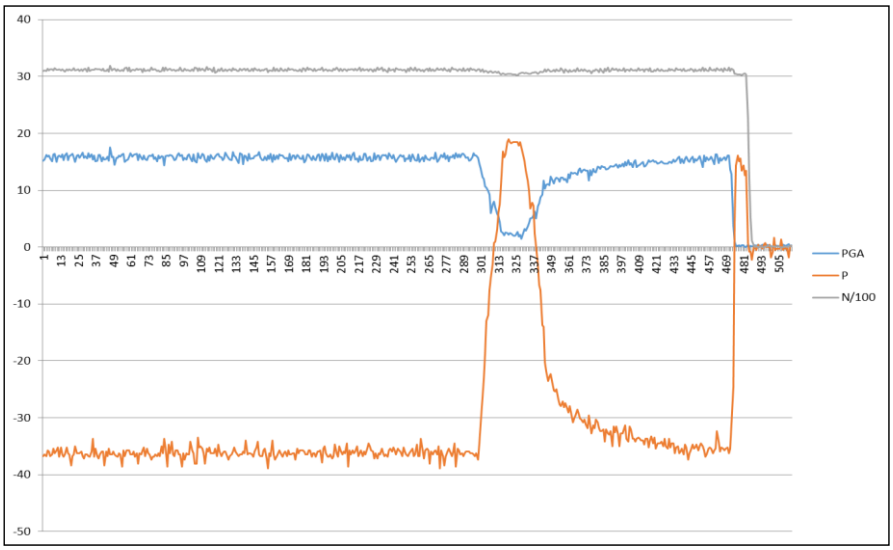

Fig. 1. The parameters of the 37 kW screw expander

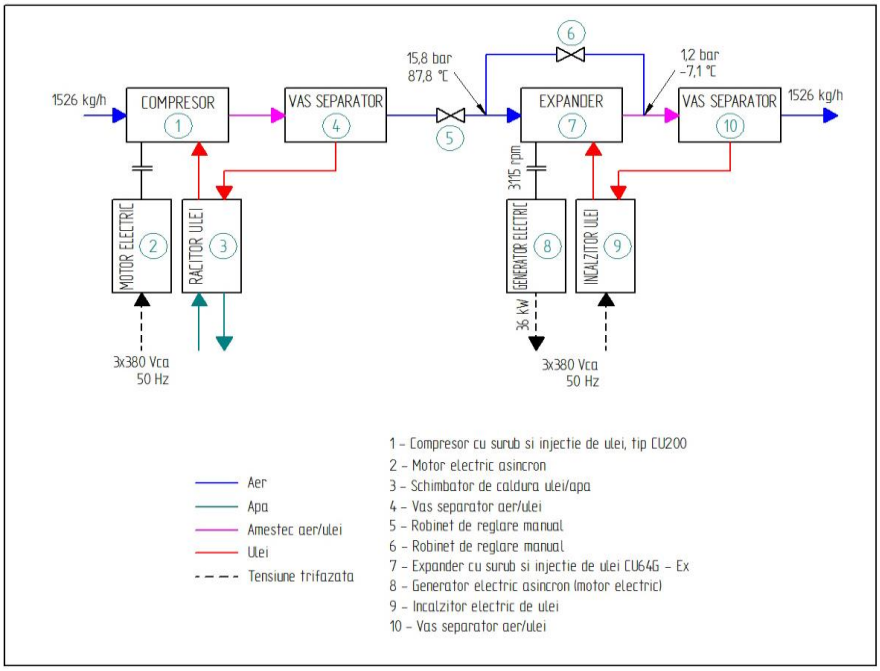

Fig. 2. General diagram of connection of the 37kW expander-generator group in the stand of INCDT COMOTI with experimental parameters

The operation of the expander - generator assembly is explained with reference to Fig.2 and to the maximum power point obtained experimentally. The air is sucked by the oil injection compressor 1. at ambiental temperature and pressure. The compressor releases an air/oil mixture of high pressure and temperature into the air/oil separating recipient 4. The hot compressed air is calibred through tap 5 at 87,8 °C temperature and 15,8 bars pressure at the expander's aspiration 7. On release out of the expander, the gas pressure has a value of 1.2 bars. The pressure difference between aspiration and discharge makes the expander to rotate and provide an air flow of 1526 kg/h. The by-pass tap 6 is partially closed so as to obtain a speed stabilization; the obtained value is 3115 rpm. The expension thus obtained determines a mechanical power at the electrical generator axis, which after its transformation by the generator produces 36 kW power. The expansion determines a decrease in gas pressure and temperature. The release temperature is being adjusted by means of warm oil used for greasing and injection by the expandor inside the expansion room. The oil heating is achieved by using an electrical heater. The expander releases an air/oil mixture out of which the oil is being separated (inside the gas/oil separator 10) only to be reintroduced into the greasing and injection circuit.

Fig. 3 The testing stand from COMOTI includes the 37kW expander– asynchronous electric generator skid

6. CONCLUSIONS

Romania's power development strategy to increase security during the electrical power supply process and to limit the power resources imports, as well as the accellerated economic development have in view the implementation of a sustained policy of power conservation though maximizing its recovery out of all available power sources. The assembly developed at National R&D Institute for Gas Turbine COMOTI Bucharest represents a new type of equipment, a novelty on the European market considering the helical expander - power generator configuration, which will have the advantages of the screw compressors: high efficiency, reduced maintanance costs due to very good reliability, few mobile parts, and last, but not the least, a competitive price [4].

Presently, the helical expander - generator group is in the final preparation stage for installation in the station.

To conclude, the turbine - generator system will be implemented inside a SRM with the aim of recovering the maximum quantity of useful energy that is available during the process.

ACKNOWLEDGEMENTS

This work was carried out within "Nucleu" Program TURBO 2020, supported by the Romanian Minister of Research and Innovation, project number PN 16.26.02.03.
The results obtained during the scientific research activity were delivered at several scientific and professional conferences both in Romania and abroad, and they materialized into an invention patent: Equipment for power production **no. 125674**, diplomas and medals received at international exhibitions:

- Equipment for power production**: IENA** , **Nuremberg 2012 - Gold medal**;
- Equipment for power production**: Eureka 2012 – Silver medal**;
- Equipement pour la production d'energie: **Geneve 2013 – Gold medal.**

REFERENCES

[1]. TOMA N., 2007; Turbina cu surub, Forumul de gaze naturale, Editia a II-a, Sibiu, Romania
[2]. TOMA N.,2009; Sistem de producere energie electrica din energia de detenta neutilizata a gazelor naturale, ROMANIA GAS FORUM Ploiesti, Romania
[3]. TOMA N., 2009, Sistem producere energie electrica, Forumul de gaze naturale Editia a III-a, Bazna, Romania
[4]. TOMA N., 2010; Recovery of the gas energies expansion by electrical power production for low gas flow,TechnoForum of OMV Petrom E&P2nd Edition: Compressors Days, Ploiesti, Romania
[5]. TOMA N., 2010; Solutie moderna de recuperare a energiei de detenta a gazelor prin utilizarea expanderelor, Drilling and production servicing seminar, Bucharest, Romania

A REVIEW OF THE TYPES OF HEAT EXCHANGERS USABLE IN CLOSED-CYCLE TURBOENGINES OPERATING AT LOW TEMPERATURE

Constantin SANDU[9], Felix ZAVODNIC[9], Mioara COSTACHE[9]

ABSTRACT: The present article is a presentation of several heat exchangers that can be used within closed cycle turboengines operating at low temperatures. In the case of closed cycle turboengines, the heat exchangers are used for the transfer of heat to the working fluid following its compression, as well as for the transfer of heat from the working fluid to an external cooling agent, these actions being necessary for resuming the engine cycle. The analysis results are useful to INCDT-COMOTI for the prospective development of turboengines that may work in a closed cycle regime at low temperatures of the engine cycle.

KEYWORDS: CO_2, CO_2 supercritic, closed cycle, low temperature.

NOMENCLATURE

H_C, kJ/kg - Variation of enthalpy with the compression evolution (inside the compressor)
H_T, kJ/kg - Variation of enthalpy with the deflection evolution (inside the turbine)
l_C, kJ/kg - Specific mechanical work with the compression evolution
l_T, kJ/kg - Specific mechanical work with the expansion evolution
p, bar - Pressure
q_1, kJ/Kg - Heat quantity introduced into the cycle
q_2, kJ/kg - Heat quantity extracted from the cycle

1. INTRODUCTION

It is known that principle I and II of thermodynamics are the basic working principles for thermal machines. Principle I establish the energy equivalence between the heat and the mechanical work, while Principle II (Carnot, 1824) indicates, on the one hand, that full transformation of heat into mechanical work is not possible, and, on the other, that the working fluid must perform within two temperature limits. This is the reason why, in the case of a turboengine working in a closed cycle (Fig. 1) it is absolutely necessary that it should contain at least two heat exchangers 1, 2 (Fig.2).

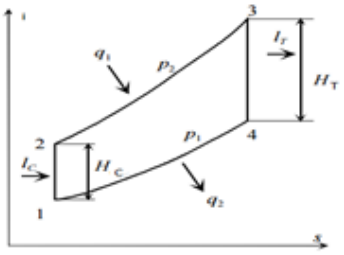

Fig. 1 Ideal Brayton Cycle

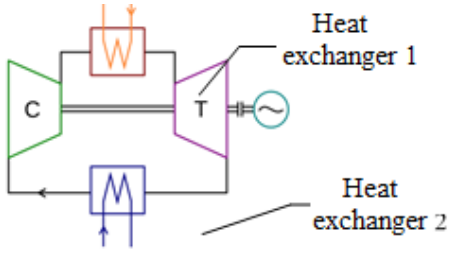

Fig. 2 Classic design of a turboengine operating in a closed cycle

[9] National Research and Development Institute for Gas Turbines COMOTI

[where q_1 and q_2 are the heat quantities introduced into/extracted from the cycle by the exchangers 1, 2; l_C, l_T-specific compression mechanical work within the compressor, and specific deflection mechanical work within the turbine respectively, and H_C, H_T-corresponding enthalpy variations; p_1, p_2-maximum and minimal pressure indices of the cycle].

2. TYPES OF EXCHANGERS TO BE USED

The heat exchangers are subdivided into surface exchangers, where heat is transferred through a high thermal conductivity wall separating the two fluids, and mixture exchangers, where the heat exchange takes place through the mixture of the fluids [1][2]. It is obvious that, as regards the turboengines operating in a closed cycle regime, the mixture aspect is not to be taken into account as the two fluids are separated. As regards the mechanics of the heat transfer within a given time, the former may be stationary (in a constant regime) or unstationary. Heat exchangers operating in a constant regime usually contain a surface separation, while the unstationary heat transfer exchangers accumulate heat during a certain time span only to release it afterwards. In the case of closed cycle turboengines, stationary exchangers are preferable as they obviously ensure a stationary function of the the turbo engine.

The heat exchange surface can be made up of concentrical pipes, that is, of a 'pipe within pipe' type, of serpentine pipes or of profiled plates, their surface being either smooth or profiled. Depending on the flow direction of the fluid along the surface, the flows may be one way ('in echicurrent'), in opposite ways ('in counter current') or complex flows may occur such as, for example, 'in cross flow', where one fluids flows perpendicularly on the other [3].

The analysis of the existent constructive solutions, and the experience gained by several research centres studying the closed cycle turboengines, reveal the fact that the most frequently used heat exchangers are those with a bundle of pipes [4] and those with plates [5]. The bundle pipes exchangers (Fig. 3) are usually used for their heat absorption supply into the cycle, while those having plates (Fig. 4) are used for their heat release capacity to the external cooling agent.

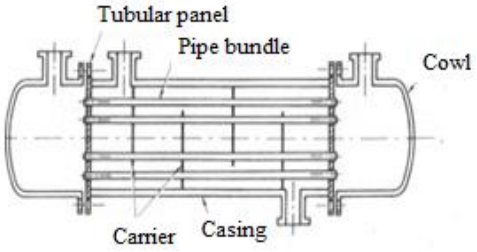

Fig. 3 Heat exchanger with pipe bundle

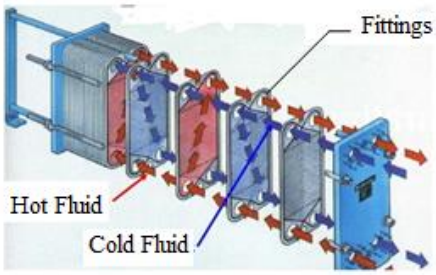

Fig. 4 Heat exchanger with plates

Bundle pipe heat exchangers are preferred, whether they use fuels that generate hot gas inside low temperature burners (wood waste, low quality coal, etc.), or solar energy (Fig. 5) [6].

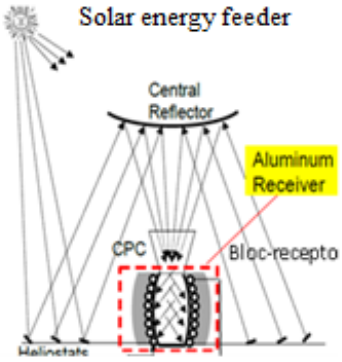

Fig. 5 Use of pipe exchangers for heat absorbtion

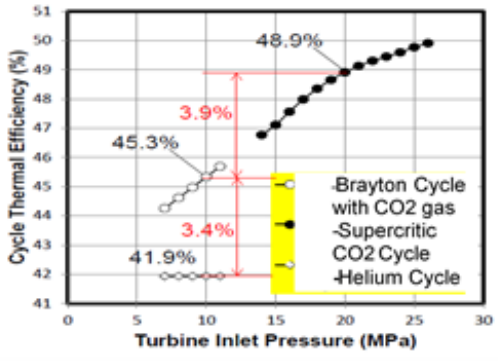

Fig. 6 Use of pipe exchangers for heat release

As regards the field of closed cycle turboengines, both theoretical and experimental research begun over a decade ago by the Toshiba Corporation has led to the development in 2016 of the first prototype turboengine (25MW) operating in closed cycle and using supercritic CO_2, which was installed in Texas, SUA [7].

The reason why supercritic CO_2 is being used is that a high thermal output (50%) of the cycle is obtained considering the fact that the maximum temperature of the cycle is low (600°C), and up to 65%, in the case of higher temperatures of the cycle, such as up to 1200°C [8]. The pressure used within the cycle were of 300 bars, that is 10 times higher than the pressure used in the common Brayton cycles.

Obviously, the use of such high-pressure indices requires special precaution measures during the design of the turboengine.

Early experiments undergone at the Sandia labs, USA, indicated that the closed cycle turboengines using supercritic CO_2 develop quite serious problems as regards the wearing of their installation components, and of their heat exchangers in particular (Fig.7,8) [9].

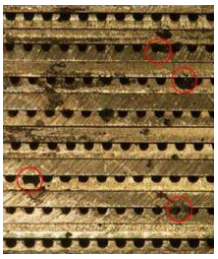

Fig. 7 The abrasion inside 3D printed the heat exchangers using supercritic CO_2

Fig. 8 The abrasion of the compressor stator within turboengine using supercritic CO_2

Fig. 7 proves that the 3D printed heat exchanger presents high erosion areas determined by the supercritic CO_2. Besides, although the supercritic CO_2 is a high chemical inertia gas, when it is used at high pressure and along with the lubrification oils, it unexpectantly produces tars that block the chanels of the exchanger. Moreover, Fig.6 [6] indicates that the cycle output working on gasous CO_2 is only a few per centage lower than the cycle output with supercritic CO_2. That is why the solution that uses gasous CO_2 becomes a serious competer for supercritic CO_2 because in the case of the gasous CO_2 cycle the same pressure is used as currently employed within turboengines (up to some dozen bars) and not extreme pressure as in the case of the supercritic CO_2 cycle (up to some hundred bars).

3. CONCLUSIONS

The present article has analyzed the working principles and the constructive solutions for the heat exchangers that may be used inside the closed cycle turboengine circuit operating at low temperatures.

In the case of the closed cycle turboengines, the heat exchangers represent a highly important equipment necessary for the heat transfer to the working agent following its compression, and from the working agent to an external cooling agent after its deflection within the turbine, both actions being a must for the resuming of the engine cycle.

Bibliography study has revealed that the international trend in the field of closed cycle turboengines construction is biased towards the use of plate or pipe bundle heat exchangers.

An important conclusion is that the solution that uses gasous CO_2 is easier and achievable with much lower costs for COMOTI, as compared to the solution that uses supercritic CO_2. Emplyment of supercritic CO_2 as a thermalagent implies the use of highly eroded heat exchangers by the high density (similar to that of liquids) supercritic fluid.

When using CO_2 gas, sealing the tiles can be used for pipe gaskets sealing the tiles from the deck. These gaskets from metal pipes may be manufactured in COMOTI welding electrode in argon nefuzibil and their use allows reaching temperatures of 500 ... 600°C, higher than in the case of using rubber linings thermistor.

ACKNOWLEDGEMENT

This work was carried out within “Nucleu” Program TURBO 2020, supported by the Romanian Minister of Research and Innovation, project number PN 16.26.01.05.

REFERENCES

[1]. Schröder K., 1971, *Centrale termice de mare putere* (traducere din lb. germană), vol. 3, Ed. Tehnică Bucureşti, 339
High Power Thermic Stations (translated from German), Vol. 3, Bucharest, Technical Print House,
[2]. Carabogdan I.G. ş.a., 1978, *Instalaţii termice industriale*, Editura Tehnică, Bucureşti, 115-119
[3]. STAS 8435-75 Utilaj pentru industria chimică. Schimbătoare de căldură. Clasificare
[4]. STAS 8475-83 Utilaj pentru industria chimică. Schimbătoare de căldură cu manta şi fascicul tubular rigid. Tipuri şi dimensiuni.
[5]. http://www.scritub.com/tehnica-mecanica/Constructia-schimbatoarelor-de82239.php
[6]. Muto Y. ş.a.; 2014, Comparison of Supercritical CO_2 Gas Turbine Cycle and Brayton CO_2 Gas Turbine Cycle for Solar Thermal Power Plants, The 4th International Symposium - Supercritical CO_2 Power Cycles, Pittsburgh, Pennsylvania
[7]. https://phys.org/news/2014-10-first-of-a-kind-supercritical-co2-turbine.html/
[8]. Ahn Y. ş.a.; 2015, Review of Supercritaical CO_2 Power Cycle Technology and Current Status of Research and Development, Advanced Institute of Science and Technology, Korea
[9]. Kruizenga A., Fleming D., Carlson M., Anstei M., Supercritical CO_2 Heat Exchanger Fouling, Sandia National Laboratory, SAND2014-17502

OPTIMISING LOW SPEED DYNAMIC BALANCING OF HIGH SPEED ROTORS

Alexandru TUDORACHE[10], Robert ISAC[10], Emilian TOMA[10]

ABSTRACT: The research conducted revealed some particularities of the rotors manufactured and/or assembled at INCD Turbomotoare COMOTI. Different phenomena were encountered, named, and described, using data recorded while dynamically balancing the rotors, like the phenomena where a rotor spins with progressively lower amplitude of vibration when increasing the rotation speed (named self-centering phenomena), to a point where the rotor stabilises, and the phenomena where the heavy point of a specific correction plane appears to move angularly while balancing at progressively increased speeds (phenomena usually encountered in the case of flexible rotors). The recorded data was used to create six graphs that give a clear image of a rotors' behaviour on a specific range of speeds. After gathering a lot of experimental data, certain patterns emerged that helped formulate a balancing procedure based on these graphs. The procedure was tested successfully and it immensely reduced the time required for dynamic balancing with better results while operating in normal conditions (lower levels of measured vibration of the machinery), at the designed nominal speed.

KEYWORDS: dynamic balancing, high speed rotors.

1. INTRODUCTION

This paper is about the research conducted regarding the optimization of low speed balancing of rotors that operate at high speed within all activities conducted at INCD Turbomotoare COMOTI: rotor assemblies for centrifugal compressors, rotor assemblies for jet micro-engines, high speed pinions and gears, rotors for test rigs, etc. The vast majority of all published papers regarding dynamic balancing mention that it is one of the fundamental requirements for any machinery to work correctly for a long period of time and that the residual unbalance is one of the key factors that lead to machinery failure or destruction. These facts have lead researchers around the world to dedicate a lot of time and effort in developing both the process of dynamic balancing (theories, methods, recommendations that, in time, were all used to create an international standard for dynamic balancing) and the machinery used (different types categorized by working principles, type of balancing, shaft position, suspension type, etc.).

2. PROCEDURE

In this paper, key observations regarding the placement and several phenomena (encountered while balancing different rotors) will be described. These finding were used to optimize the process of dynamic balancing by better determining the position of the heavy point, location where mass must be removed to reduce unbalance to acceptable limits, and reducing the time it takes to achieve this acceptable limit for residual unbalance.

2.1. Proper placement of rotor

Due to the configuration of some rotors, it may be very difficult to place the rotors on the balancing machine. It is very important that the rotor be placed on two of its flat surfaces, even if all geometric tolerances are met. The small errors greatly influence the measured values for amplitudes of vibration.

[10]National Research and Development Institute for Gas Turbines COMOTI, Bucharest, Romania

For example, we measured the amplitudes of vibration for the rotor of a jet micro-engine (~284 mm total length and 1.1 kg weight), which was so small it barely fit on the balancing machine. We tried two configurations, one intentionally wrong, just to see the differences (Fig. 1), at the speed of 3050 RPM.

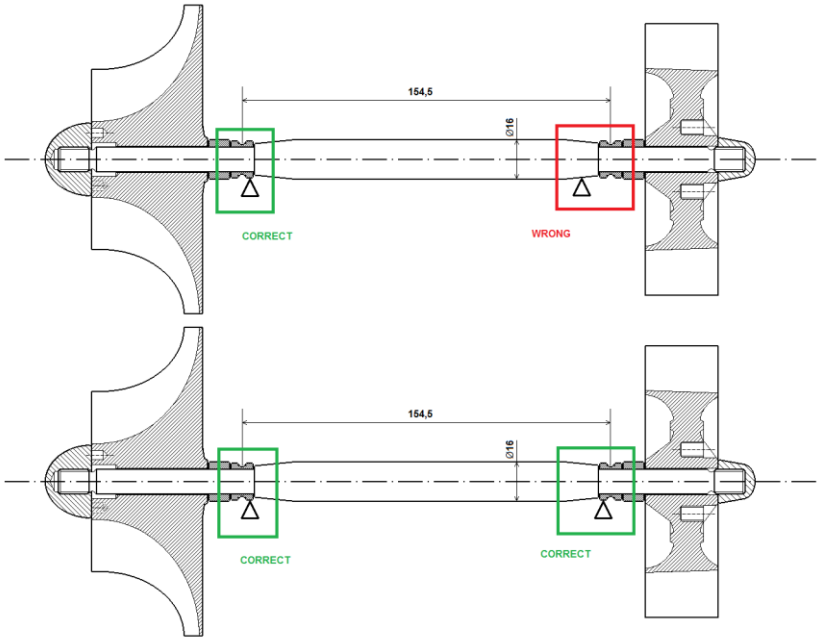

Fig. 1 Jet micro-engine rotor placement

The first placement involved using the inner ring of the ball bearing in the left plane, and the cone surface on the turbine side in the right plane, while the second placement, and the correct one, involved using both ineer rings of the ball bearings. Even though the geometry was within specified tolerances given by the designer, the measured mean amplitudes of vibration were 4 µm in the left plane and 11.5 µm in the right plane, for the first run, a lot higher than the values measured for the second run 0.5 µm in the left plane and 9 µm in the right plane. The difference is substantial, given the small size and mass of the rotor, while the remaining amplitude of vibration of the right plane is another subject of discussion not relevant to this paper but, in short, it was due to the turbine having an axial run-out.

1.1. Auto-centering phenomena

We name this phenomena so, because when measuring the amplitude of vibration over a certain range of speeds, at specific intervals, we notice a drastic reduction in vibration to a level where the rotor stabilizes. For example:a pinion for a centrifugal compressor stage (Fig. 2), a screw compressor gearbox gear (Fig. 3) and the rotor assembly of a gear test rig (Fig. 4).

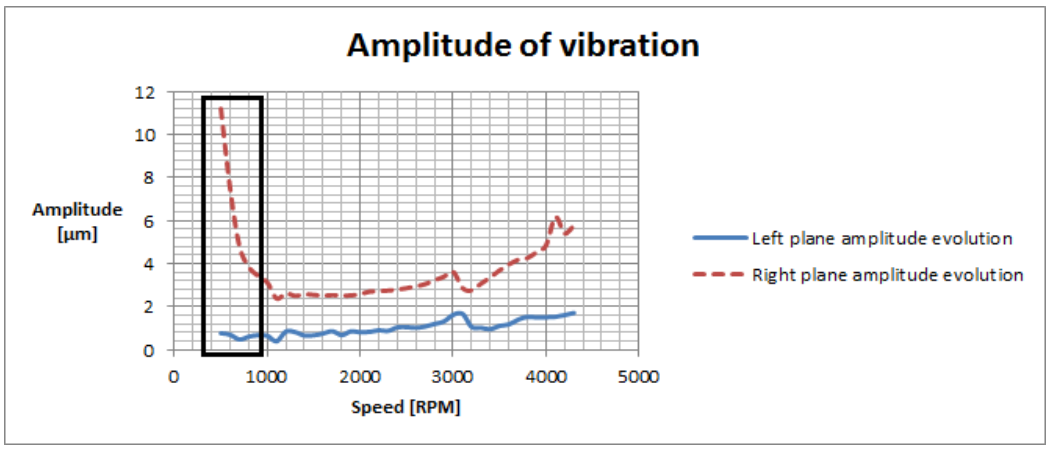

Fig. 2 Amplitude of vibration of a centrifugal compressor stage pinion

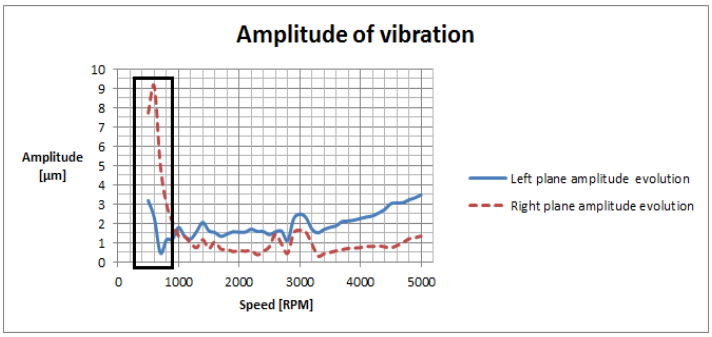

Fig. 3 Amplitude of vibration of a screw compressor gearbox gear

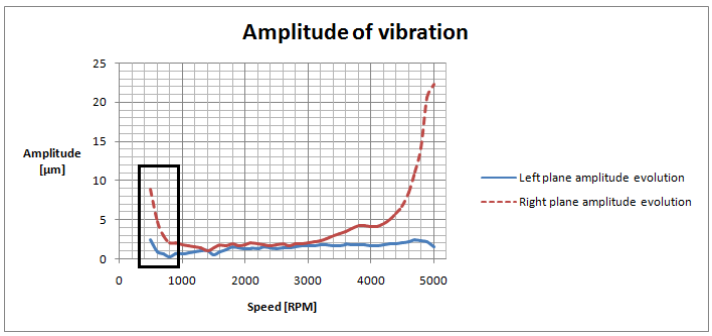

Fig. 4 Amplitude of vibration of the rotor assembly of a gear test rig

1.1. Migration of the heavy point phenomena

This phenomena is named so, because in the graphs it appears that while the speed at wich we measure the amplitude of vibration increases, the position in polar coordinates of the heavy point changes, allways in the same direction as the rotation (in our case, counter-clockwise). After the auto-centering phenomena fully manifests (Fig. 5, section A) and the rotor stabilizes (Fig. 5, section B), we notice an area of the graph where the amplitude of vibration starts to increase (Fig. 5, section C). This phenomena appears especially in the case of flexible rotors.

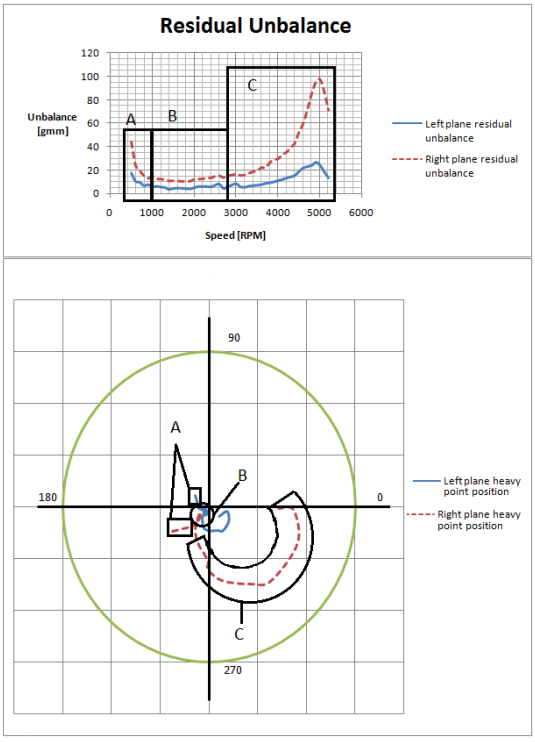

Fig. 5 Heavy point position corelated with balancing speed in the case of a rotor assembly of a gear test rig

This observation is immensely important, especially when balancing the rotor because the position where material needs to be removed changes with the speed of balancing.

All the rotors that have been tested were dynamically balanced and the amplitude of vibration was again measured. The values obtained were within calculated tolerances for residual unbalance.

2. CONCLUSIONS

With the knowledge and experience obtained by observing these phenomena and by balancing the rotors where they manifested, we have concluded that the speed of balancing must be chosen between the speed where the auto-centering phenomena fully manifests and the speed where the heavy point starts migrating due to the increase in measured amplitudes of vibration caused by the elastic deformation of the rotor. These observations have led to the creation of a balancing procedure that uses knowledge of previous rotors to better determine the position of the heavy point and reduce the time taken for dynamic balancing.

ACKNOWLEDGEMENT

This work was carried out within “Nucleu” Program TURBO 2020, supported by the Romanian Minister of Research and Innovation, project number PN 16.26.03.05.

REFERENCES

[1]. Neville F. Rieger, 1989; Balancing of rigid and flexible rotors, Shock and Vibration Information Center;
[2]. Dynamic Balancing Handbook Form #2049,1990; IRD Mechanalysis Inc.
[3] Radet M.,2008; Dinamica Masinilor III (Dynamics of Machinery III), Ed. Printech, Bucuresti;
[4]. Yoon S.Y. et al., 2013; Control of Surge in Centrifugal Compressors by Active Magnetic Bearings, Advances in Industrial Control, Chapter 2, Springer, London;
[5]. Ref.doc.MI 104 - Nota Tehnica – Consideratii privind echilibrarea rotoarelor rigide (Techincal Note – Considerations regarding rigid rotor balancing), Mobil Industrial AG, 2009;
[6]. Ref.doc.MI 105 - Nota Tehnica – Echilibrarea dinamică a rotoarelor flexibile (Technical Note – Flexible rotor balancing), Mobil Industrial AG, 2009;
[7]. Gunter E.J., Charles Jackson, Rotordynamics, Chapter 3, Balancing of rigid and flexible rotors;
[8]. ISO 1940-1:2003, Mechanical vibration - Balance quality requirements for rotors in a constant (rigid) state;
[9]. ISO 11342:1998, Mechanical vibration - Methods and criteria for the mechanical balancing of flexible rotors;
[10]. ISO 19499:1998, Mechanical vibration - Balancing - Guidance on the use and application of balancing standards.

COMOTI Capabilities & Expertise

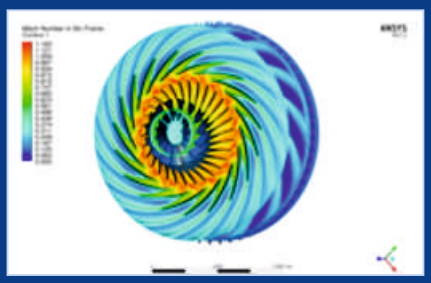

Centrifugal rotor CFD applications.

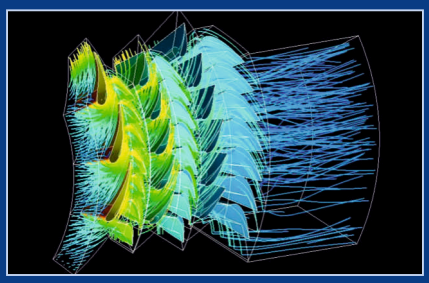

Gas turbine CFD applications.

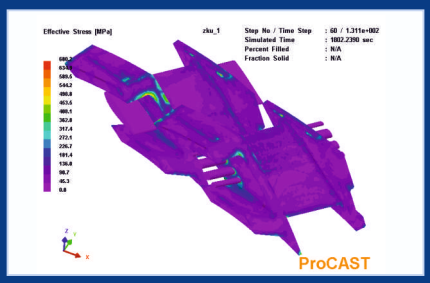

Casting FET applications.

Planetary gear box 3D design.

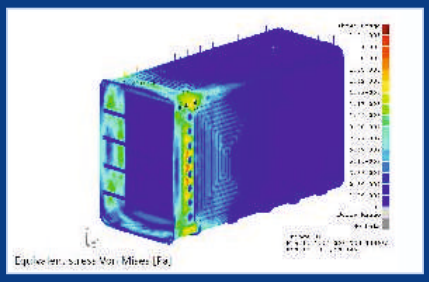

FEA low pressure thermal box.

Gas turbine engine 3D design.

HAAS grinding CNC.

Centrifugal rotor on MCNC.

Centrifugal rotor.

Alien condition test facility.

DELTA 34.04 CMM.

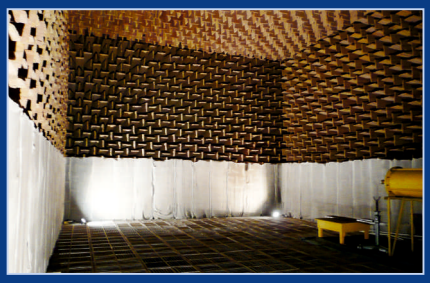

Anechoic chamber.

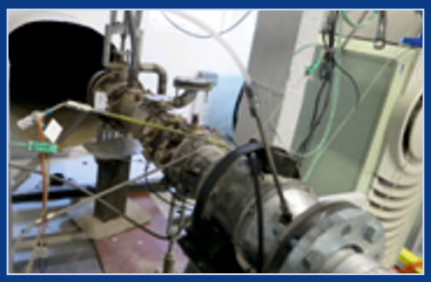

Combustion test rig.

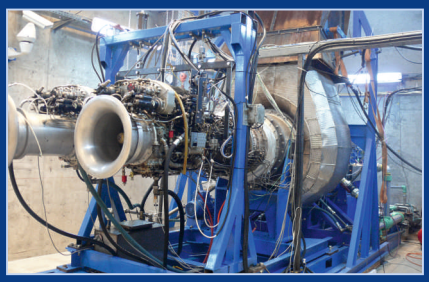

Gas turbine engine test rig.

Micro turbjet for target plane.

Screw compressor skids station.

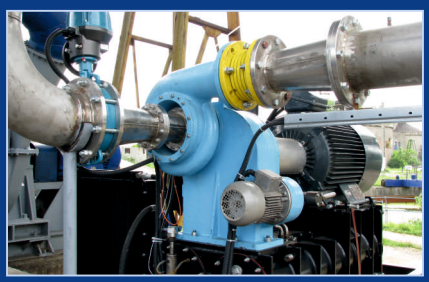

Centrifugal blower skid.

Centrifugal compressor skid.

COMOTI

The only specialized company that integrates such activities as

scientific research,
design,
manufacturing,
testing,
experimental activities,
technologic transfer and innovation

in the field of aircraft and industrial gas turbines and high speed bladed machinery.

220D Iuliu Maniu Ave., 061206 Bucharest, ROMANIA,
P.O. 76, P.O.B. 174
Phone: (+4)021/434.01.98, (+4)021/434.02.31, (+4)021/434.02.40
Fax: (+4)021/434.02.41, e-mail: contact@comoti.ro

www.comoti.ro